INFORMATION TO USERS

This manuscript has been reproduced from the microfilm master. UMI films the text directly from the original or copy submitted. Thus, some thesis and dissertation copies are in typewriter face, while others may be from any type of computer printer.

The quality of this reproduction is dependent upon the quality of the copy submitted. Broken or indistinct print, colored or poor quality illustrations and photographs, print bleedthrough, substandard margins, and improper alignment can adversely affect reproduction.

In the unlikely event that the author did not send UMI a complete manuscript and there are missing pages, these will be noted. Also, if unauthorized copyright material had to be removed, a note will indicate the deletion.

Oversize materials (e.g., maps, drawings, charts) are reproduced by sectioning the original, beginning at the upper left-hand corner and continuing from left to right in equal sections with small overlaps.

Photographs included in the original manuscript have been reproduced xerographically in this copy. Higher quality 6" x 9" black and white photographic prints are available for any photographs or illustrations appearing in this copy for an additional charge. Contact UMI directly to order.

Bell & Howell Information and Learning
300 North Zeeb Road, Ann Arbor, MI 48106-1346 USA
800-521-0600

Design and Development of a Laboratory Scale Twin-Wire Sheet Former

Christopher J. Hammock
Department of Chemical Engineering
McGill University, Montreal

September 1998

A thesis submitted to the Faculty of Graduate Studies and Research in partial fulfilment of the requirements of the degree of Master of Engineering

Abstract

A laboratory sheet former using the twin-wire concept has been designed and constructed. It is capable of simulating a wide range of industrial papermaking conditions and can generate a pressure profile very close to that of an industrial machine. The machine has three components: the headbox section, the drainage section and the sheet pick-up section. All three sections are activated and brought up to operating speeds independently, with the headbox flow being diverted back into a reservoir. Once all systems are running at their operating conditions, the headbox flow is diverted to form a jet and steady-state sheet forming occurs for a certain period. The sheet and seven white water streams are collected during operation.

The system is currently able to simulate the papermaking process up to the beginning of the vacuum drainage section; the sheet which it creates has a consistency in the vicinity of 11%. Mass balances of better than 95% have been achieved for both water and fibre. The magnitude of the pressure profiles generated has been measured or calculated. Continuing work will bring the sheet consistency into the 15% to 20% range; once this is attained, an efficient tool to optimize wet-end chemistry will be available.

Résumé

Une formette de laboratoire a été développée selon le concept double-toile. Sa conception permet de simuler une multitude de conditions industrielles de fabrication du papier et de reproduire un profil de pression similaire à celui d'une machine à papier. La machine comprend trois sections: la caisse d'arrivée, la section de drainage et la collecte de la feuille. Les trois systèmes sont indépendemment mis en marche. Lorsqu'ils ont atteint les conditions d'opération, la suspension est détournée vers la caisse d'arrivée pour former un jet de pâte. La production de la feuille en régime permanent prend place pour une certaine durée. La feuille et l'eau blanche sont recueillis au cours de l'essai.

La feuille produite par cette machine a une consistance d'environ 11%, ce qui correspond à la consistance de la feuille à la section des boîtes à vide du procédé industriel. Des bilans massiques ont montré que plus de 95% des fibres et de l'eau sont récuperé en fin d'essai. Le profil de pression le long de la section de drainage a été mesuré ou calculé. On vise la production d'une feuille ayant une consistance de 15 à 20%. Cette machine rendrait alors possible l'optimisation de la chimie du bout humide.

Acknowledgements

The author would like to acknowledge the following individuals for their assistance over the course of this project: Ivan Pikulik, Robert Daunais, Daniel Gilbert, Robert Gooding and especially Bob Stone and his staff, all Paprican employees, for their valuable advice and efforts in the design and construction of the apparatus; Mario Rouleau and his staff for the wonderful machine work performed in constructing and modifying the apparatus; Professors Derek Gray, Murray Douglas and Theo van de Ven of McGill, for their helpful comments; all my office mates and coworkers for their patience and good will, especially when I was running experiments; my family, for their genuine, if naive, interest in the work I'm doing; and finally, my supervisor, Professor Gil Garnier, for all the support, guidance (ask for or not) and freedom he has given me in doing my work. Without the contributions of any of these people, this work would not have been possible.

The author would also like to acknowledge the support lent by the following institutions: the Pulp and Paper Research Institute of Canada, for major financial and technical support; the Paper Industry Management Association, for financial support; and Johnson Wires Inc., for providing parts and technical support for the project.

Table of Contents

List of Figures

1. Introduction

Over the past several years, the paper product industry has been going through a period of adaptation, one that is likely to continue for years to come. Over the past thirty years, paper machine design has switched from using horizontal, single fabric machines to using faster and more efficient vertical, two-fabric machines [1]. Also, environmental and economic concerns are both pushing the industry to accept two major process changes: the switch from using virgin fibre as a raw material to using recycled paper products; and the reduction of paper mill effluent by treating process water and reusing it in the process.

1.1. The History of the Paper Machine

Original paper machines were horizontal; this type of machine, generically called a "fourdrinier" after one of its original financiers [2], is shown schematically in Figure 1. The pulp is poured out of the headbox over a thick, woven fabric, or "wire". The moving fabric travels away

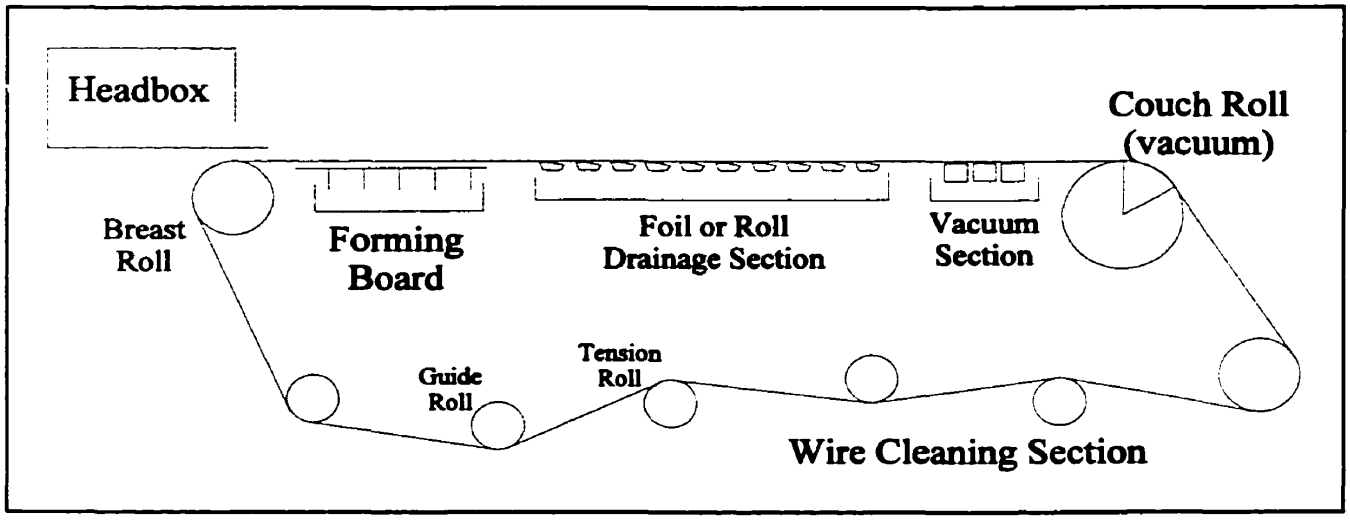

Figure 1: Schematic of a fourdrinier machine

from the headbox, the source of the pulp. It first passes over the forming board, where the slurry stabilizes and water begins to drain out of it through the fabric; fibres remain behind and start to form the sheet. Further drainage is effected by table rolls, foils and vacuum boxes. Thus formed, the sheet is then transferred to another carrying medium for further water removal by pressing and by drying. However, the fourdrinier has several limitations. Fines, tiny slivers that break off the fibres, tend to get washed out of the bottom face of the sheet as drainage occurs. Fines are important for the optical, printing and strength properties of the sheet, so the bottom face will differ significantly in these properties from the top; this phenomenon is known as "two-sidedness". Also, the speed of a fourdrinier machine is limited; if the sheet travels too fast, it can be easily disrupted as it forms. A high speed is desirable in order to maximize production; however, a higher machine speed also requires a longer drainage section in order for the drainage time of the slurry to remain the same. Machine lengths of up to one hundred metres are possible.

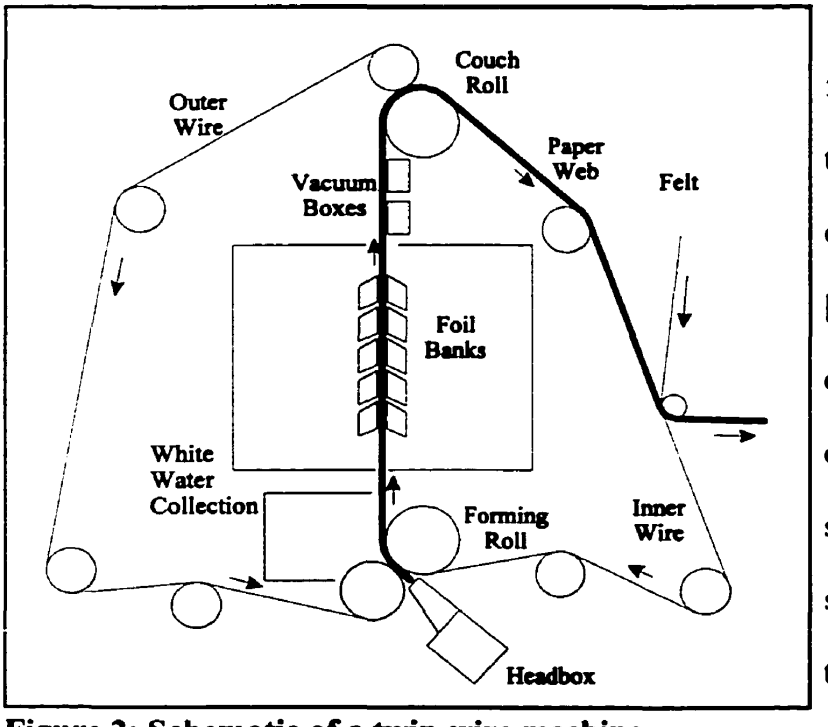

Figure 2: Schematic of a twin-wire machine

These limitations of the fourdrinier lead to the development of the twin-wire paper machine, an example of which is shown in Figure 2 [3]. With this design, the pulp is directly injected between two converging wires under tension. Held securely between the two wires, the sheet can travel at velocities several times that of a fourdrinier without being disrupted. Similarly, water can

drain through both faces simultaneously, so two-sidedness is reduced or eliminated and the drainage rate is increased. Many fourdrinier machines are still in use today; however, virtually all new machines being constructed are twin-wire machines.

1.2. Environmental Concerns

The reuse of paper fibre is not a terribly new concept and has been in practice for many centuries. Large scale adoption, however, is fairly recent in North America, as legislation and public opinion have called for more recycling of paper. Organized collection of waste paper has made its use as a furnish more practical and more affordable. It also has the advantage of easy availability in urban centres, so that paper mills needn't transport their fibre from distant pulp mills. However, the use of recycled fibre does have certain problems. Recycled fibres can carry contaminants from their previous application into the papermaking process. These can be physical contaminants, such as staples and plastic windows, or chemical contaminants, such as ink, glossy coatings, and property enhancing additives (strength additives, waterproofing agents, etc...). An additional series of unit operations is generally required in a mill to clean the recycled fibres before they are made into a usable pulp. Often, the cleaning process is imperfect and some of these contaminants are carried over into the sheet forming section.

Original paper mill designs had fresh water being drawn to suspend fibres in order to form a pulp. This water would then be removed as the pulp was converted into a sheet. The water would carry with it large quantities of chemicals left over from the pulping process and chemicals added to enhance the properties of the final sheet. This pollutant-laden stream would then be discharged into a nearby river. Modern environmental laws no longer allows this. Such laws, as well as the potential for the reclamation of heat and materials (fibres and additives) and the potential reduction

of fresh water consumption have motivated paper mills to try recycling. The first attempt at solving the problem, which is still widely used, was to simply treat the water before discharging it [4]. Such treatments range from settling tanks for separating solids from liquids, to biological lagoons for degrading organic contaminants. The next generation of effluent treatment was to reduce, or eliminate altogether, the effluent stream. The same water treatments are used, but some or all of the treated water is then recycled back into the process. Perfect treatment of the water is not economical, so some degree of contaminant carryover often occurs.

1.3. An Evolving Industry

Many more chemical additives are being used to manufacture high-performance, specialty grades of paper. This trend, compounded by the two process changes discussed above, means that papermaking process chemistry is becoming more and more significant. The composition of the chemical mixture being circulated through a paper mill can have drastic effects on the efficiency of operation and the quality of the final product. Therefore, research in the area of papermaking chemistry is extremely important today, in order to better understand the interaction between various additives and to develop additives that complement one another. In order to test such additives and study the general effects of process chemistry, we must be able to accurately study the sheet forming process. However, real paper machines operate on an enormous scale and at immense speeds. Industrial mill production has a value on the order of tens of thousands of dollars per hour, so they are normally unavailable for short term research operations. Smaller scale pilot machines exist, but purchasing time on these is expensive and not always possible; these machines are also inflexible in their operating conditions. The goal of this project is to go one step smaller yet, to develop an apparatus capable of simulating the industrial sheet forming process, but at the laboratory scale.

1.4. Project Objectives

The principal objective of this project is to develop an apparatus capable of accurately simulating the sheet forming process that takes place on an industrial papermaking machine. It is important to note that there already exist several devices capable of producing a paper sheet in the laboratory. However, none of these are able to do so in a way that properly reproduces in a controlled manner all the mechanisms of pulp flow and water drainage that occur industrially [5]. Thus, it is not just the *final product* that we are trying to simulate, but also the *process* whereby this product is manufactured. This is important because many papermaking chemistry problems must be defined in terms of turbulence, shear, pressure profile, water drainage rate and other factors which, themselves, depend very much on process conditions. Thus, in order to properly study the physical and chemical behaviour of a papermaking system, one must be able to simulate *all* the process conditions.

With these considerations, the specific project objectives can be laid out as such:

1) Design and construct a laboratory scale apparatus capable of accurately simulating the sheet forming process that occurs on an industrial paper machine. The entire process, from the pulp jet to the collection of the wet sheet coming off the machine should be so simulated.

2) Experiment with the apparatus in order to verify its operability, to study and optimize its sheet forming capability, and to have it produce a wet sheet comparable to that of an industrial machine.

2. Literature Survey

2.1. Pulp Drainage and Sheet Formation

The process whereby a pulp slurry is transformed into a moist sheet has been a subject of serious study for almost fifty years. Some of the earliest work on pulp drainage was carried out independently by P.E. Wrist [6] and by G.I. Taylor [7],[8] in the 1950's. Much of their effort was dedicated to the analysis of drainage as carried out by table rolls and foils, the principal drainage elements used on fourdriniers. A sketch of these devices can be seen in Figure 3. In particular, they were interested in characterizing the suction profile generated by these devices and the effect that they had on the sheet. As shown in the sketch, both these devices produce a suction zone as their surface diverges from the wire; it is

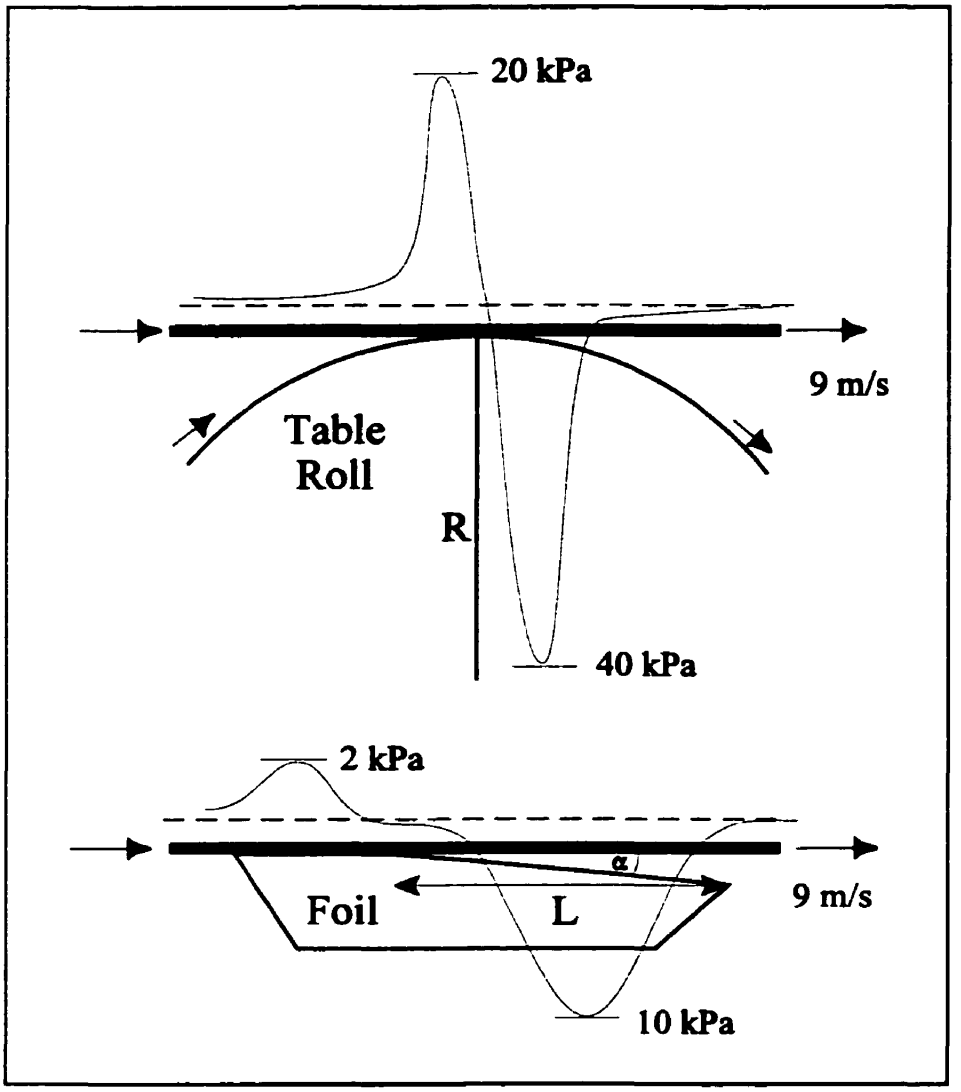

Figure 3: Pressure profile of a table roll and a blade on a fourdrinier machine

this suction zone that effects the removal of water from the pulp. Estimating the shape and magnitude of this suction envelope and relating it to theoretical expressions was the researchers' main activity. Taylor derived a differential equation to describe the pressure profile of a forming roll as:

$$\frac{x^2}{2R} = \int_0^x \frac{\phi(s_y)dy}{\sqrt{U^2 + \frac{2}{\rho}[s(x) - s_y]}} \qquad \text{(Eq. 2.1.1)}$$

where x is the wire direction, U is the wire speed, R is the roll radius, and ρ is the density of the drainage water. The suction experienced at the surface of the wire is s_y. The suction along any streamline that emerges from the wire and then continues downwards around the roll is given by s(x) as a function of the distance along the machine direction; $\phi(s_y)$ is the drainage rate of water through the wire as a function of applied suction, s_y, and must be found experimentally. Solved numerically, this equation generates a curve similar to that in Figure 3, with a peak value of

$$s(x) = \tfrac{1}{2} \rho U^2 \qquad \text{(Eq. 2.1.2)}$$

For a typical wire speed of 9m/s, this would produce a peak dewatering vacuum of 40 kPa. However, because of the strong dependance on velocity, table rolls became a liability as machine speeds increased with technology; the suction they generated became so strong it would damage the web. Therefore, foils were developed as an alternative for high speed machines.

Foils generate a similar curve, modelled by Taylor as

$$\frac{S}{\frac{1}{2}\rho U^2} = \frac{2a\left(1 - (x/L)^{1/a}\right)}{\left\{1 + \frac{a}{1-a}\left(\frac{x}{L}\right)^{1/a}\right\}^2} \qquad \text{(Eq. 2.1.3)}$$

where $a = \alpha\mu/k\rho U$, α is the blade angle and L is the blade length. As α increases, the peak of the suction envelope increases but its width decreases. Maximum flow out of the sheet can be attained by optimizing these two parameters and the wire speed. Suction from a foil is generally lower (on the order of 20 kPa) but because they are much smaller more of them can be placed along the forming section to produce the same drainage.

It is also interesting to note that upstream of each drainage element, an upwards pressure surge *into* the wire is generated. It is this pressure surge that is responsible for "sheet hopping", another phenomenon that disrupts the sheet when fourdrinier machines are run too fast.

More recently, a great deal of work has been performed in characterizing the dewatering generated by twin-wire machines. The drainage profile of a typical twin-wire roll-blade former producing 7 tonnes per day of product is shown in Figure 4 [9]; the "consistency" (the mass fraction of solid fibres in the suspension or in the web) of the sheet between units is also shown. Of particular interest is the dewatering effected at the foils and at the forming roll; interest lies in characterizing the pressure profile generated at these drainage points. Vacuum boxes, although equally important to the process, are of less interest as their vacuum level can be easily measured and controlled. As can be seen in Figure 4, most of the water is removed from the pulp in the forming section. However, the last

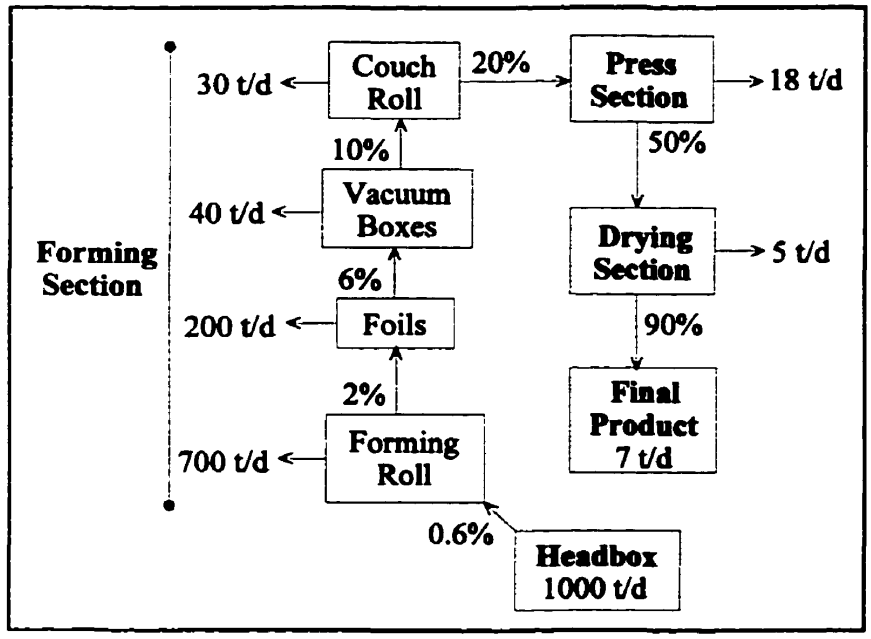

Figure 4: Drainage profile of a twin-wire machine

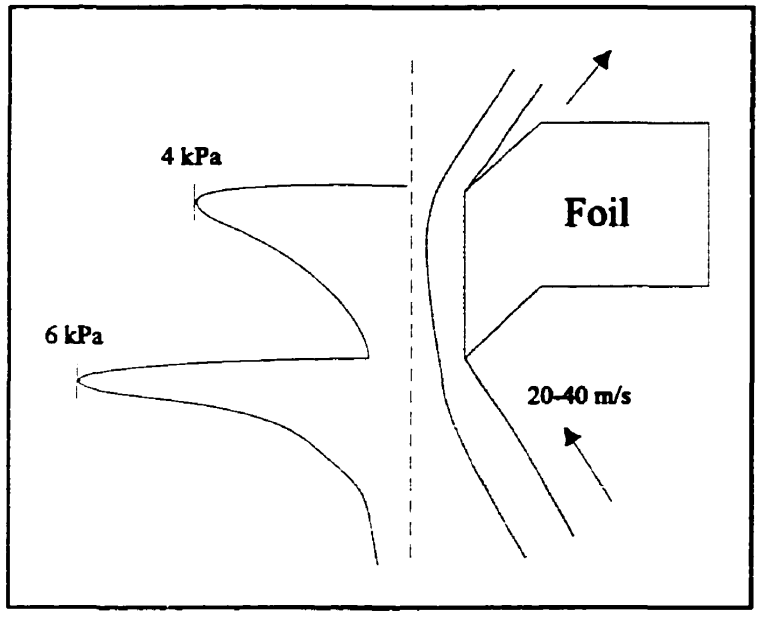

Figure 5: Pressure profile of a foil on a twin-wire machine

remnants of water must be removed from the sheet in the press section and the dryer section. In the press section, the sheet is held between water-absorbing sheets of felt and passed between several pairs of heavy rolls. The pressure exerted by the rolls on the sheet drives out water, which is then absorbed by the felt. In the dryer section, the last water is evaporated out of the sheet by some method of heating.

A great deal of work has been carried out recently in the study of blade dewatering, particularly by Zhao and Kerekes[10] and by Zahrai, Bark and Norman[11] . As can be seen in Figure 5, the pressure pulse generated by a foil on a twin-wire machine differs from that on a fourdrinier. The pressure within the wires is caused by the tension in the wires as they are pinched against the front and rear edges of the foil. Essentially, the pulp is sandwiched between the wires as the foil impinges upon them. Since the pulp is subjected to two edges, the leading and trailing edge, it actually undergoes two pressure pulses. At the leading edge, both wires are open to the atmosphere, so dewatering can easily occur through both faces. However, at the trailing edge, the foil itself blocks water migration through the inner wire, so dewatering takes place primarily through the outer wire. As shown, the sharp leading edge of the foil also serves to scrape accumulated water off the surface of the inner wire (referred to as "doctoring"). Water which isn't doctored off can be pulled between the wires and the blade. In this confined space, the tension in the inner wire can drive the water back through the wire and into the pulp; to minimize this effect, blades are designed

to optimize doctoring. Some surface water is also thrown off the outer wire by centrifugal forces as the wires curve around the foil.

Zhao and Kerekes assumed a thin blade (having only one pinch point) and solved the continuity and Navier-Stokes equations for the pulp system. They were able to derive a model that matches a single peak from Figure 5:

$$p(x) = T(\alpha_1 + \alpha_2)\frac{G_1 G_2}{G_1 - G_2}\left[e^{G_2 x} - e^{G_1 x}\right] \qquad \text{(Eq. 2.1.4)}$$

where

$$G_1 = \frac{k_2 \rho V_0}{H_0}\left(1 + \sqrt{1 - \frac{2H_0}{k_2^2 \rho T}}\right) \quad \text{and} \quad G_2 = \frac{k_2 \rho V_0}{H_0}\left(1 - \sqrt{1 - \frac{2H_0}{k_2^2 \rho T}}\right)$$

and x is the machine direction, α_1 and α_2 are the leading and trailing wire wrap angles, T is the (identical) tension in both fabrics, k_2 is the permeability of the web and fabric, ρ is the density of the suspension, V_0 is the wire speed, and H_0 is the thickness of the slurry before the blade. The model shows the observed phenomenon that as wire velocity, wire tension or wrap angle increases, so does the magnitude of the pressure spike.

Experimental measurements were made on a pilot machine with Pitot tubes drilled along the length of the blades to obtain an experimental pressure profile. A leading wrap angle of zero degrees was used in order to generate a single pressure spike at the back of the blade. Experiments varying the wire speed, outer wire tension and departing wrap angle showed the behaviour expected from Figure 5 and Eq. 2.1.4. The inner wire tension was held constant because the inner wire exerts very little pressure upon the suspension.

Green[12] has derived a simplified theoretical model for the drainage effected by a foil. By ignoring the dynamic nature of the system and performing a static force balance between the wires and the blade, he was able to find an expression for the average drainage pressure as a function only of the wire tension and the wrap angle of the wire around the foil:

$$\int_{-L}^{+L} p(s)ds = T\alpha_{Tot} \qquad \text{(Eq. 2.1.5)}$$

The first term is the pressure integrated along the length of the blade, which is equal to the product of the outer wire tension and the sum of the leading and trailing wire wrap angles. Dividing the integral by the length of the blade gives the average dewatering pressure. The results obtained from the model agreed with experimental results to within a few percent at low drainage rates, increasing to a 10% error at high drainage rates; this deviation is attributed to the dynamic effects which were ignored. Because these dynamic effects were ignored, no effect of wire speed is included.

Drainage around a forming roll is more difficult to model, because it occurs via two mechanisms: the impact of the pulp jet upon the wires and the pressure exerted by the wires as they pull the pulp around the forming roll[13]. Martinez[14] has investigated the drainage induced by the wire wrap. He derived a theoretical drainage model but obtained his pressure profile experimentally; a plot of this is shown in Figure 6. Zone A is where the pulp jet emerges from the headbox and strikes the wire, creating a large pressure

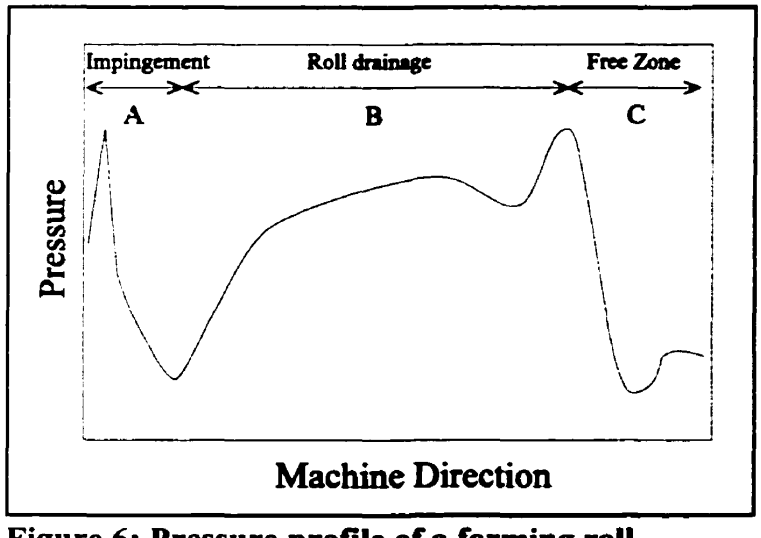

Figure 6: Pressure profile of a forming roll

spike (not included in the model). Zone B is the forming length where the wires wrap around the forming roll and most of the water is squeezed out; here, a large pressure envelope is created, reaching a maximum near the end of the contact region. Zone C is the distance after the forming roll, where the wires are free and the pressure drops down to normal. The magnitude of the pressure envelope in zone B is often estimated using the expression $P = T/r$, where T is the tension in the wires per unit width and r is radius of the roll; a more rigorous discussion of this will be given later. Martinez showed this expression to match his experimental data to within approximately 10% at the peak of the pressure envelope.

Very little study has been devoted to the drainage effected where the pulp jet first impinges upon the wire, or to the drainage carried out by vacuum boxes. The pressure profile of both these situations can be arrived at through theory or engineering, and will be discussed later for the system under study.

The pressure profile, although a very important part of the sheet forming equation, is still only the driving force for sheet dewatering. The actual dewatering mechanism and the resistance to drainage are also equally important, as is the sum of these three pieces, the rate of water removal. A great deal of qualitative and quantitative work has been performed over the past fifty years since the time of Wrist and Taylor. This work has been thoroughly and concisely reviewed by Meyer[15], Kershaw and Cutshall[16] and especially by Parker[17]. Most of this work was on determining the physical mode of water removal and in measuring the effects of assorted variables on the resistance to drainage and, hence, on the drainage rate.

There are two extreme theoretical mechanisms for the dewatering of pulp. Both cases, *filtration* and *thickening*, are shown schematically in Figure 7. In filtration, it is hypothesised that as water is removed from the pulp and forced through the wires (by whatever means), the fibres that

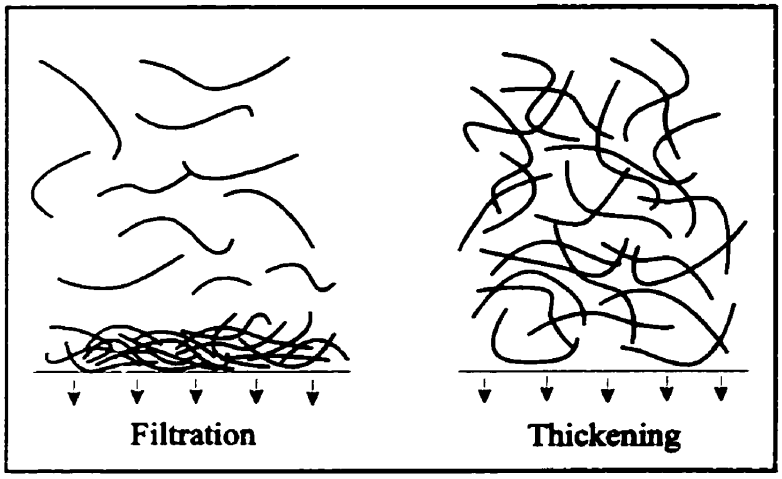

Figure 7: Illustration of drainage mechanisms

were suspended in that volume of water deposit on the surface of the wire. They thus form a second, separate "sheet" phase of much higher fibre concentration than the rest of the pulp slurry. Two such sheets form, one on each wire. As more water is removed, more fibres deposit, so that over time these sheets of fibres becomes thicker and denser, thus presenting a greater resistance to further dewatering of the pulp; at the same time, the pulp phase shrinks in size. It is assumed that the concentration of suspended fibres in the remaining pulp slurry remains constant at the same value as the pulp had upon entering the drainage section. Eventually, the slurry phase disappears and the two sheets merge into one.

Thickening is the opposite view, in which the pulp slurry remains as one phase throughout the process. As water is removed, the fibres that were suspended in that volume are redispersed throughout the remaining slurry phase. Therefore, as dewatering progresses, the concentration of fibres in the slurry increases, until such time as all free water has been removed and the pulp slurry has been homogeneously transformed into the wet sheet.

Predictably, neither of these two mechanisms has been shown to operate exclusively [17]. Experimental evidence shows a combination of them, wherein fibres that were suspended in removed water are both deposited and redispersed, so that the sheet forms separate from the pulp phase, but the fibre concentration of the pulp phase also increases. However, this evidence also shows that the filtration mechanism tends to dominate. Sheet forming conditions also play a large role in determining the drainage mechanism. Paper machine technology has been advancing so

rapidly over the past fifty years that machine speeds have been increasing linearly from less than 1m/s to well over 40m/s in some applications[18]. Modern paper machines are not only much faster, but also shear the surface of the pulp slurry on two sides rather than just one; consequently, there is much more turbulence and, hence, more mixing (for a wire speed of 10m/s and a slurry thickness of 3mm, the Reynold's Number of the flow is around 30 000). Thus, the thickening mechanism tends to be more prevalent on modern machines than it was on older ones.

The resistance to drainage has traditionally been one of the most prolific fields of study in papermaking engineering. This is simply because of the myriad of variables that affect it. Every batch of pulp has a different drainage resistance, because the pulp specific surface area, fibre length distribution and fibre quality differ from one batch to the next. Even in batches from the same fibre source, these three characteristics will differ slightly. These characteristics, as well as the processing performed on the pulp before sheet forming, and the additives used in the pulp, affect how the pulp will drain. The principle factor in determining pulp drainage is the quantity of "fines" in the pulp. Fines are tiny slivers that are broken off from the fibres during processing; they can account for up to 60% of the material by mass in mechanically produced pulps, but rarely exceed 10% in chemically produced pulps[19]. By bridging the fibres together in the final sheet, they impart much higher strength to the sheet; by scattering incident light, they augment the brightness and opacity of the sheet. However, by plugging up gaps between the fibre they also impair drainage of the pulp. Much of papermaking chemistry has been devoted to augmenting retention of fines in the sheet for their beneficial effects, while simultaneously trying to minimize their hindrance to drainage. The flocculation state of the fines and fibres is also important. If the material is clumped together it will hold onto water very strongly; if it is mostly dispersed, water will flow much more easily. The

flocculation state of the pulp depends strongly on the composition of the pulp and the local flow conditions.

Another less glorified resistance to drainage is the wires themselves. Of course, they are required to support the forming sheet, but they inhibit the flow of water to some degree. A compromise is generally required, between maximizing drainage and minimizing the loss of fibres and fines through the wires. Development of fabric weaves and fabric materials is a small part of papermaking engineering research. As a general rule, resistance to drainage increases along the sheet forming section. Initial drainage resistance is due solely to the wire. As the wet sheet forms, it begins to impose an additional resistance to water migration. Likewise, as the slurry thickens, it becomes more difficult to remove water from it. Therefore, drainage rate tends to decrease along the forming section, as illustrated by Figure 4.

The drainage rate is usually quantified using Darcy's Law:

$$v = \frac{dP/dx}{\mu R} \qquad \text{(Eq. 2.1.6)}$$

where v is the fluid velocity through a porous medium, dP/dx is the pressure gradient through the medium, μ is the viscosity of the filtering liquid and R is the (empirical) resistance to flow of the medium. R is not a simple constant, and is often modelled using the Kozeny-Carman analysis:

$$R = \frac{kS_v^2(1-\varepsilon)v}{\varepsilon^3} \qquad \text{(Eq. 2.1.7)}$$

where S_v is the specific surface area of the fibres, v is the specific volume of the fibres, ε is the porosity of the mat and k is the Kozeny factor. The Kozeny factor is a function of ε, which is itself a function of the pressure gradient. These relationships must be determined experimentally.

Because of the assumptions made in deriving it, Darcy's Law only technically applies to creeping flow through a porous medium (when the Reynold's Number based on the characteristic length of the pore structure is less than 1). However, its partially successful application to sheet forming and general ignorance of the exact patterns of flow through the sheet structure have combined to make the theory widely used in this field. Generally, a measured flow rate is correlated to a measured or theoretical driving force (pressure profile) and a measured or theoretical resistance value, with one or more other factors being included, depending on the researcher. Until recently, most of this was done empirically; however, much current research is focussing on the theoretical mass transfer and fluid mechanics that govern the sheet forming process.

2.2. Laboratory Sheet Formers

Simulation of the sheet forming process is necessary for many branches of pulp and paper research, particularly the study of wet-end papermaking chemistry. This is the study of how the properties and composition of the pulp affect the sheet forming process and the final product. Such simulation is also important for the studies discussed in the previous section, those investigating the nature of how the sheet actually forms. In the case of wet-end chemistry, an accurate simulation is less important than a repeatable simulation. The *relative* performance of, for example, two different types of pulp in the same experiment is more important than the *absolute* performance of either one. On the other hand, sheet forming research requires a very accurate simulation of the sheet forming process. For this reason, most such studies are carried out on industrial machines or the pilot machines owned by research organizations. Current laboratory sheet formers are simply incapable of accurately simulating the industrial sheet forming process.

The Handsheet Maker

The most commonly used laboratory sheet former is the handsheet maker[20]. A schematic of this device is shown in Figure 8. With the valve closed, the water column is filled up to the level of the drainage mesh. The chamber above the drainage mesh is filled with the pulp being studied, diluted to one tenth the concentration of industrial pulp. The valve is then opened and the water in the column rushes out, drawing behind it the water in the pulp. The fibres are deposited on the drainage mesh as the water drains out. They form what is referred to as the "handsheet". The handsheet is then pressed and heated dry. The properties of the handsheet can then be studied, usually in comparison to those of other handsheets formed with a different pulp.

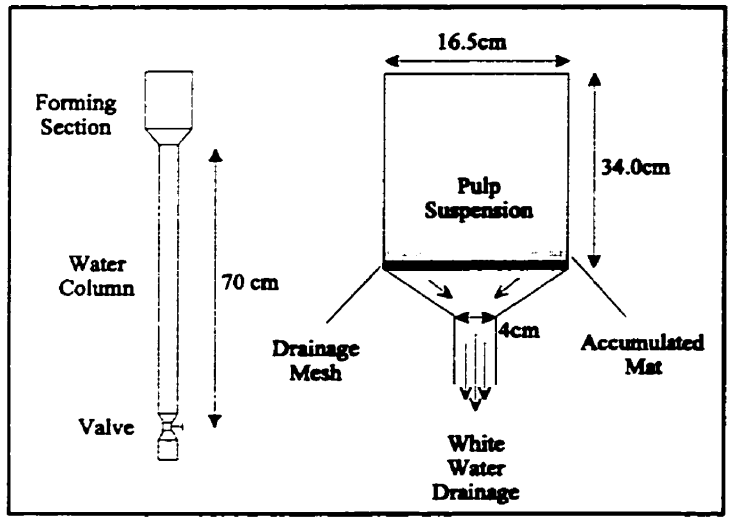

Figure 8: Schematic of a handsheet maker

The handsheet maker has many strengths. Perhaps most importantly, it is an internationally recognized test method. As it is relatively inexpensive, almost all papermaking chemistry labs have a handsheet machine; therefore, it provides a common reference for all researchers. The procedure for making a handsheet is straightforward and quick, and thus highly reproducible. Different researchers from different labs can confidently compare results as long as the same handsheet making protocols are followed. This ubiquitousness also means that it is difficult for any other sheet forming device to gain popularity - many have tried, but none has yet supplanted the handsheet maker as the primary lab tool of papermaking researchers.

The handsheet maker also has several drawbacks. As mentioned, the pulp is far more dilute than industrial pulp, so its drainage behaviour is very different from that in industry. Collision kinetics between fibres and various other components are completely different. Similarly, the drainage rate on a handsheet maker is much smaller than that on an industrial machine; the time it takes for the handsheet to form can be up to several seconds, whereas the residence time of the sheet in the forming section of a paper machine is a fraction of a second. The conditions in the handsheet maker are very static and gentle, whereas pulp in a real machine undergoes a great deal of shear and turbulence[21] from the passage through the headbox and the wild ride between the wires; this not only affects the flocculation state of the pulp, but the orientation of fibres in the sheet as it forms. The dewatering force to which the pulp is subject in a handsheet maker is the weak, constant hydrostatic pressure of the water column. An industrial machine subjects the pulp to a series of intense pressure spikes and envelopes which alternate with periods of simple atmospheric pressure; this causes the sheet structure to form, break up and rearrange many times, which has severe consequences for the final sheet. In the handsheet maker, the web forms gradually and cleanly. The formation time, flow conditions and pressure profile all strongly affect the final structure and the sheet properties that depend on the structure; this makes it difficult to draw any conclusions regarding industrial behaviour from experiments made with a handsheet maker.

The Formette Dynamique

Attempting to overcome the limitations of the handsheet maker, several manufacturers and research groups have come up with devices capable of generating a paper sample by more representative means. The most visible result of this work is the Formette Dynamique, developed at the Centre Technique du Papier in Grenoble, France during the early nineteen-sixties[22]. A

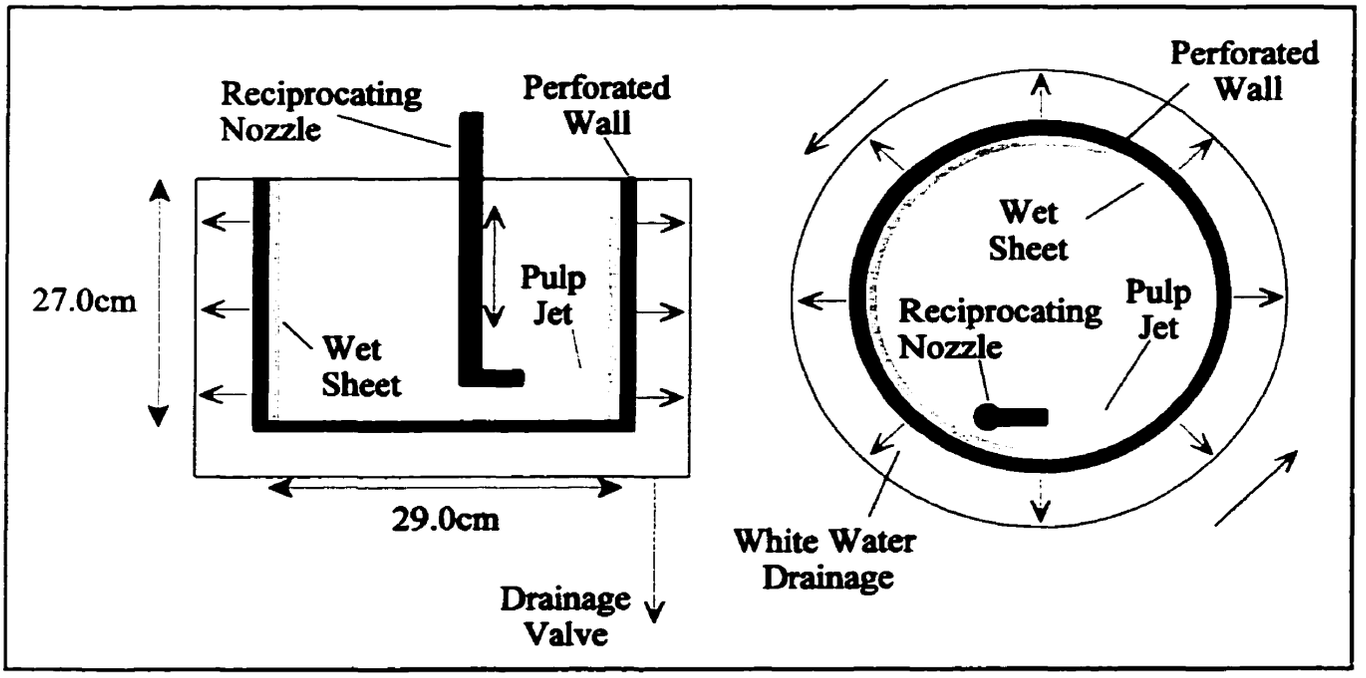

Figure 9: Schematic of a Formette Dynamique

schematic of this device is shown in Figure 9. The forming chamber rotates rapidly to produce a centrifugal dewatering pressure; the wall is perforated and surrounded by a second stationary chamber that is emptied by a valve in the bottom. Inside, the perforated wall is lined with a section of removable fabric not unlike the wire of an industrial machine. With the drainage valve closed, a layer of water is sprayed onto the wall in order to fill the stationary collection chamber just to the level of the rotating wall. The pulp is then sprayed over the fabric; the nozzle sweeps up and down to deliver a uniform layer of pulp. Once the pulp layer has been delivered, the drainage valve is opened and the water layer drains out. Without the water layer to hold it in place, centrifugal acceleration causes water to migrate out of the pulp and to pass through the fabric, through the perforated wall and into the stationary chamber to be drained away. The fibres remain behind, forming a wet sheet on the fabric.

This process provides more turbulence and shear due to the high speed of the pulp spray and the pulp striking the moving wall. The velocity differential between the jet and the wall also allows

fibre orientation in the sheet, just as is seen on industrial machines[23]. Also, real pulp of the same consistency used industrially can be fed into a formette dynamique. However, the sheet forming process involved is still very different from industry. The pulp is allowed to build up slowly on the surface of the fabric and to form a uniform structure before it is drained, very unlike the instantaneous dewatering that takes place on a real machine. When drainage does finally take place, it takes on the order of a few seconds to complete.

Researchers at CTP were able to reasonably simulate the production of newsprint, typing paper[24] and board[25]. Physical properties of the sheet that depend on fibre orientation (such as strength and tearing properties) were shown to be much closer to the industrial product than those sheets produced on static lab formers. However, no study of the retention of various components of the pulp was performed, nor were the surface properties of the sheet (such as smoothness or basis weight uniformity) shown to be any better than that obtained from a static former. Attempts have been made to relate sheet forming variables on the Formette Dynamique to equivalent machine variables in industry, in order to draw conclusions regarding the process rather than just the product[26]. This has met with limited success.

There have been many other commercial machines which attempt to recreate industrial conditions, but none of these has been accepted by the research community. The problem lies in improving the performance of the sheet former enough to justify the increased complexity of design and operation. No lab former thus far has even attempted to simulate the two-directional drainage of twin-wire machines, a technology which has raised the bar for lab formers even higher.

3. System Development

3.1. System Objectives

The global objective of this project is to develop a laboratory scale device capable of accurately simulating the formation of a wet sheet as it takes place on an industrial paper machine. There were several key elements in such a device that needed to be addressed:

Twin-Wire Design: Virtually all modern paper machines use the twin-wire configuration, yet no previously designed lab instrument simulates this two-directional drainage. Many instruments have used centrifugal acceleration or hydrostatic pressure as the driving force for drainage, which necessarily limits drainage to one direction. The resultant sheet structure and properties are very different from the real product. It was decided, therefore, that our apparatus must be capable of draining the sheet through both faces.

Drainage Profile: Most other lab devices use a single drainage process to form the sheet, whereas an industrial machine uses several. This is done because different drainage processes have different properties. For example, impingement drainage on a machine can remove very large volumes of free water, while blades and vacuum boxes are able to remove smaller volumes of the water which is bound up tightly between the fibres. There is no single drainage device which is able to efficiently remove all the water without disrupting the web. Consequently, the sheet undergoes a series of pressure and vacuum pulses of increasing magnitude over the course of its formation. This fluctuating pressure profile also affects flocculation behaviour of the pulp as it is being drained and, hence, the final structure of the wet sheet. It was decided that a series of different drainage

elements be designed into the apparatus, both to provide more efficient drainage and to provide the variable pressure profile.

Operating Speeds: This encompasses several related process parameters, particularly the pulp flow rate, pulp linear velocity leaving the headbox and wire velocity. The pulp flow rate and the wire velocity determine the basis weight (fibre mass per unit area of sheet) of the final product. The difference between the pulp velocity and the wire velocity determines the degree of fibre orientation in the sheet and, thus, the paper structure; therefore, this value must be accurately controlled. Pulp velocity also determines how much impingement drainage will occur where the pulp is delivered into the wires; a minimum pulp velocity is also required for the pulp jet to have enough momentum to penetrate between the wires as they wrap around the forming roll. Wire velocity has a bearing on the effectiveness of various drainage elements: a higher speed increases the magnitude of the drainage pressure of blades, but reduces the exposure time for vacuum drainage. Finally, all these variables determine the shear and turbulence experienced by the pulp as it is being delivered into the machine and that experienced by the sheet as it is being formed. Therefore, it was decided that the machine operate in a range of speed parameters similar to those seen in industry, yet still obeying the restrictions set by the relationships between those parameters.

Environmental Suitability: This device is intended to operate in a chemistry laboratory environment. Therefore, it must easily fit into such a setting. This requires that it have compact dimensions and a reasonable mass which will not need special support or accommodation. The device should also have moderate utility demands (electricity, water and air pressure, floor drains). It should not pose any significant threat to those working with it or around it, nor impose any inconvenience to other work by its presence or operation. Operation and maintenance should be as simple as possible.

Inherent in many of the criteria is the assumption that our device will be geometrically similar to an industrial paper machine. All discussion of wire velocities, pulp jet velocities and such, assumes that these industrial parameters will be mimicked (or at least analogous) on our apparatus. This is possible only because the initial brainstorming of the project finally settled on a design that has such geometric similarity. Many other design concepts were initially considered and rejected. Not surprisingly, the geometrically similar design concept was the only one to meet all the objectives of the project.

3.2. System Concept

The operating principle of the final system is that of a short term steady state. Industrial papermaking operates as a continuous process; however, such operation would not be convenient in a laboratory setting. However, for the simulation to be accurate, some form of steady state needs to be reached in order to study the drainage process without the transient effects of a start up and a shut down. In order for the data collected to be meaningful, the process must be long enough that large amounts of data can be collected.

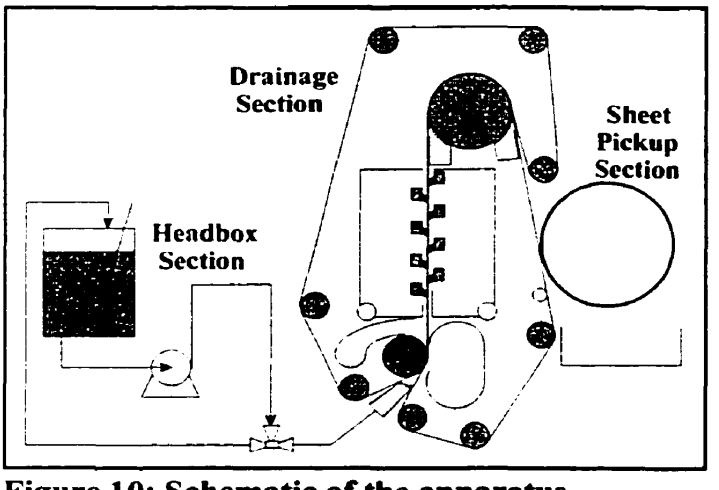

Figure 10: Schematic of the apparatus

A schematic of the system is shown in Figure 10. There are three parts to the apparatus: the headbox section, the drainage section and the sheet pickup section. The headbox section generates the pulp jet and delivers it into the drainage section. The drainage section then removes most of the water from the pulp, leaving a wet sheet of

fibres, which is then collected by the sheet pickup section. Each of these sections will be described in more detail in the following paragraphs.

3.3. Headbox Section

A schematic of the headbox section is shown in Figure 11. The purpose of this part is to generate the continuous, uniform pulp jet which will feed the sheet forming section. The four principal components of the headbox section are the reservoir, the three-way valve the headbox itself and the centrifugal pump. All components are connected with steel piping of 7.6 cm internal diameter, except the curved length from the valve to the headbox; this is 7.6 cm internal diameter rubber tubing. To start up, the valve is set to direct the flow from the pump through the recirculation line and back into the reservoir. The pump flow rate is then gradually ramped up from zero to the operating flow rate. When the drainage section is ready to receive the pulp jet, the valve is switched to direct the pump flow to the headbox line. The pulp jet quickly stabilizes and delivers a steady pulp feed into the forming section.

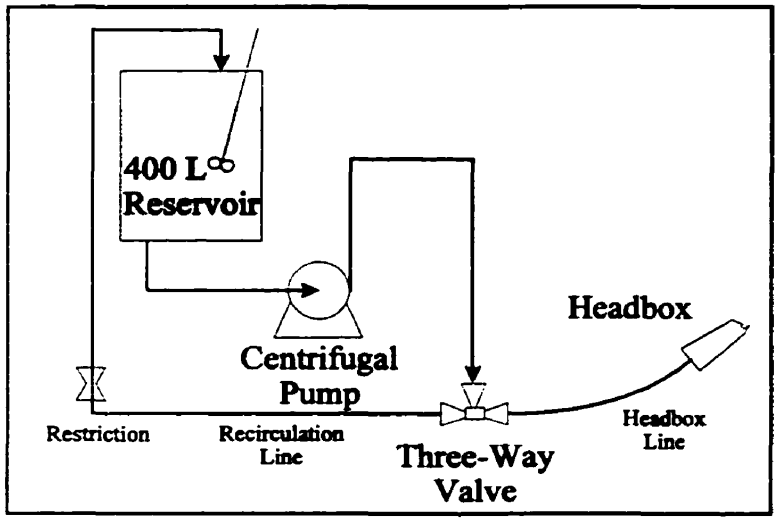

Figure 11: Schematic of the headbox section

The reservoir is a cylinder, 74 cm in diameter and 87 cm high. A schematic of the reservoir is shown in Figure 12. The bottom is a shallow cone to direct liquid to the outlet pipe. The recirculation line empties at the bottom of the reservoir so that no turbulence or entrainment of air will take place where the fluid is returned. A plastic bucket is placed below the return line to act as

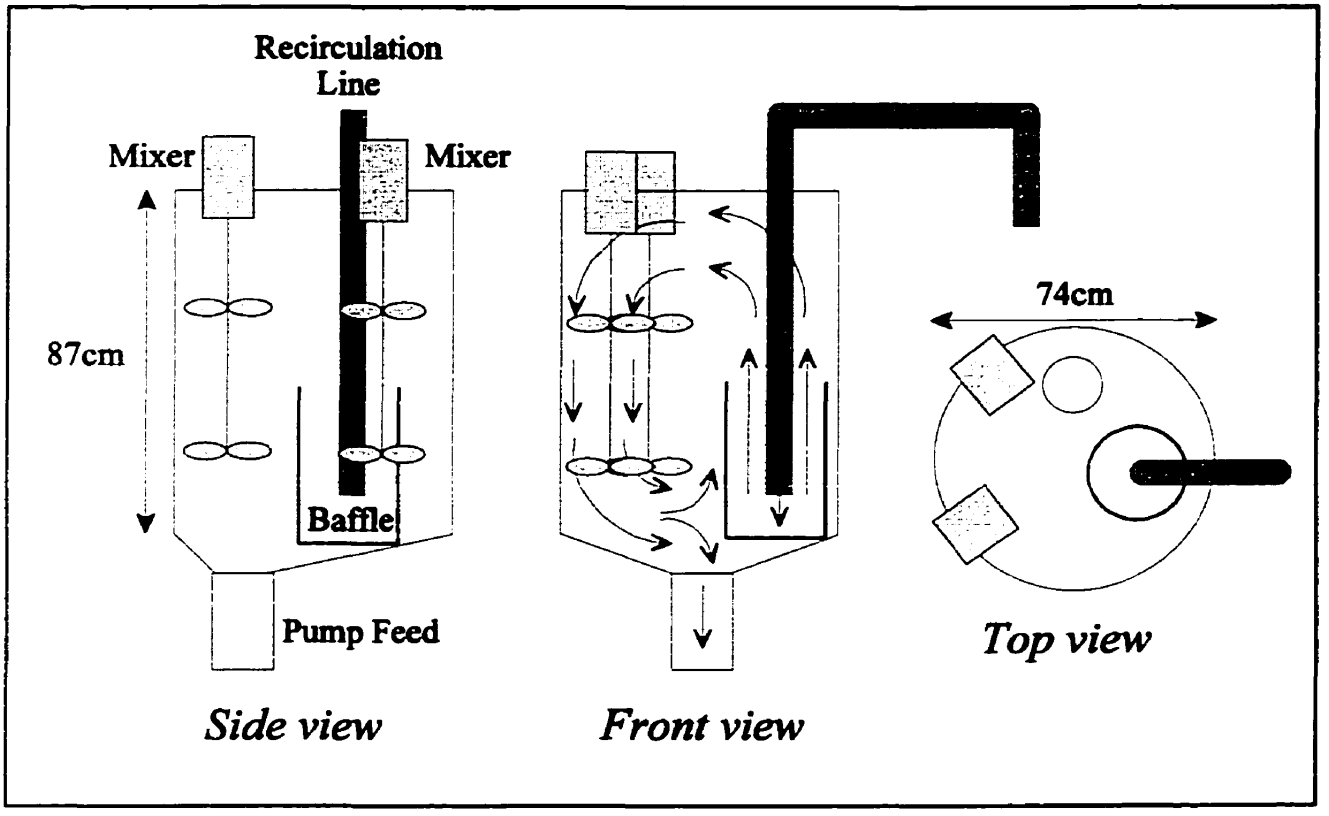

Figure 12: Schematic of the reservoir

a baffle, preventing the turbulent return flow from directly feeding the pump intake and encouraging cavitation in the pump. The baffle also promotes mixing by directing the fluid flow towards the surface. The mixers on the other side of the tank continue the circulation in the tank by driving the flow downwards. At the bottom of the tank, the flow is divided between the pump feed and that which continues around the baffle and towards the surface. When the headbox jet is being formed there is no recirculation flow, so only the mixers drive the fluid flow in the reservoir. The reservoir has three levels marked. The volume between the topmost and bottommost marks contains approximately 140 kg of pulp; the third mark is the halfway point between the first two. These marks are used during operation to control the amount of pulp delivered.

The three-way valve is pneumatically driven and has a switching time of under one second. To prevent undue stress on the pump and piping systems, a restriction is placed in the recirculation

line. The size of the restriction is calibrated to approximately balance the pressure drop through the recirculation line with that through the headbox line. Therefore, the shock to the flow system when the valve switches is minimized. Unfortunately, the contents of the headbox line, if any, are stationary. If there is water or pulp in the line, then it must be accelerated by the flow before the jet emerges; this generates a small shock as the moving pulp slams into it. If the headbox line is empty, then the flow will experience a brief surge as the empty line fills, then a shock when it hits the narrow slice opening in the headbox.

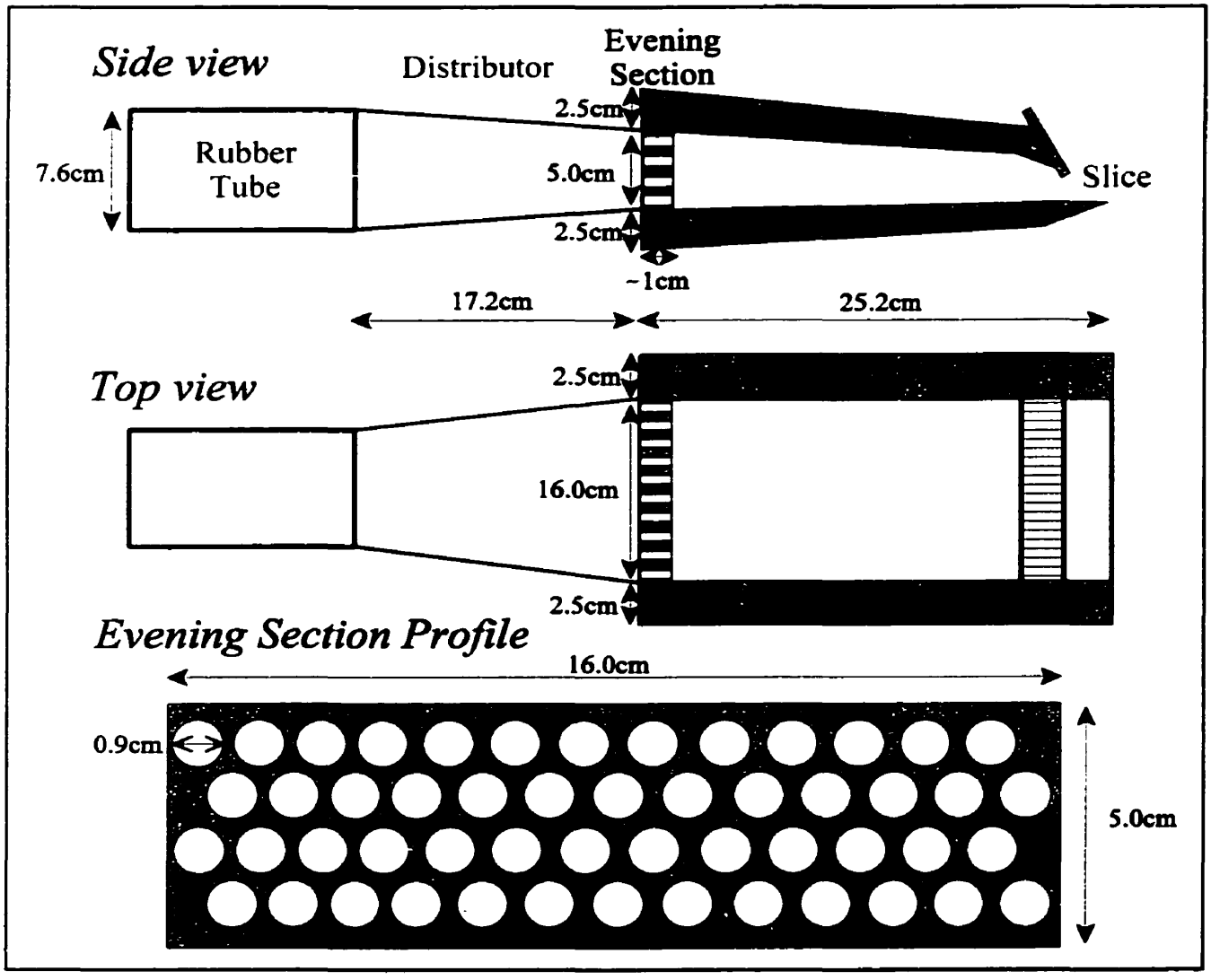

Figure 13: Schematic of the headbox

A schematic of the headbox is given in Figure 13. The pulp enters from the rubber tubing in the rear and passes through a distributor section which converts the circular tube flow into a broad, thin rectangular flow. The flow then passes through an evening section. This is a solid block with circular holes drilled through it in a honeycomb pattern. Its purpose is to flatten the parabolic velocity profile that the pulp has coming out of the pipe. It presents a large flow resistance, thus generating a large back pressure behind it. Pulp passes through all the holes at the same speed, and emerges with a uniform flow rate across the width of the headbox. The flow contracts and accelerates as it passes through the body of the headbox. It then emerges from the slice and forms the pulp jet. The slice thickness is determined by the position of the movable plate that forms the lip. It has a total range of 2 cm down to a completely closed position; however, the usual operating range is typically from 3 mm to 5 mm.

A uniform velocity profile in the jet is required in order to generate a sheet of uniform basis weight and velocity profile. If the parabolic velocity profile normal for duct flow were maintained, then the flow rate of pulp, and hence of fibre, would be significantly higher in the centre and almost zero at the edges. This would result in a parabolic basis weight profile across the width of the paper sheet. Control of basis weight uniformity is a critical requirement of headbox design. Industrial headboxes have a slice thickness around ten times ours, but a sheet width a hundred times that of ours. With such geometry, it is impossible to maintain a uniform velocity profile across the entire width of the headbox using a simple flow system like ours. Figure 14 shows two typical distributor designs used industrially[27]. The *multiple branch manifold* distributor divides the pulp flow through a series of pipe splits, recombining them just prior to the slice. As long as each split is even, the resultant jet will have a uniform velocity profile. This design was abandoned a few decades ago because it was complex to design and build and took up a great deal of space. The *cross flow*

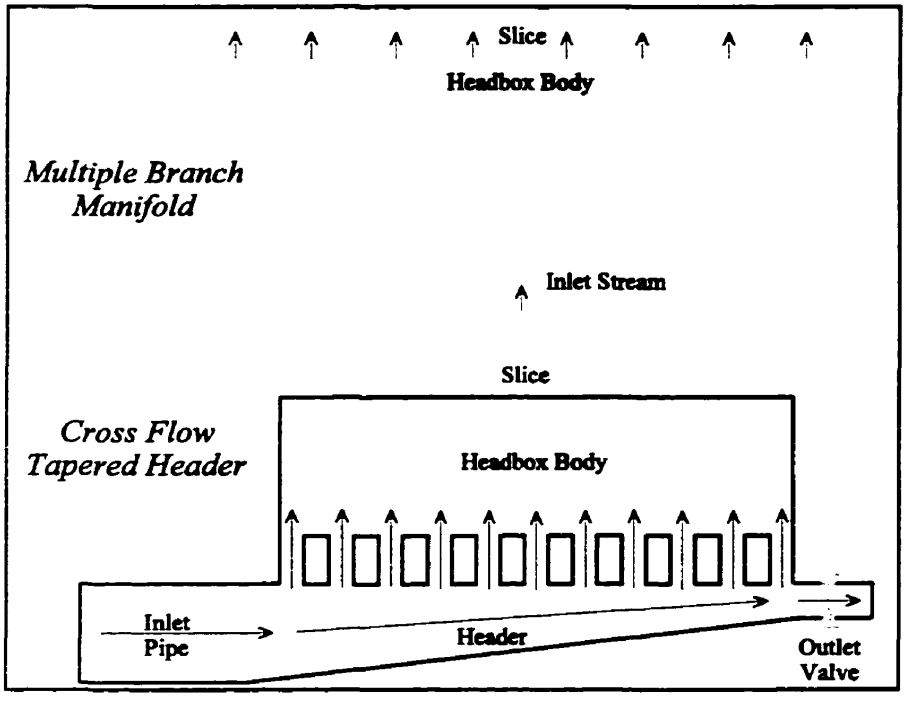

Figure 14: Schematic of industrial headboxes

tapered header distributor replaced it and is the industrial design on which our headbox is based. The pulp flows into the header and then through a series of openings similar to our distributor block and through an exit valve at the end of the header. The angle at which the header tapers is such that the pressure along the length of its body remains constant as flow is diverted through the openings. This ensures that the flow rate through each of the openings will be identical. The flow rate through the exit valve can be controlled to adjust the pressure profile along the length of the header, and thus the flow profile across the headbox. With all the openings allowing the same flow rate of pulp, the jet that forms from these flows will have a uniform velocity profile. Fortunately, our jet has a much lower aspect ratio, so maintaining a uniform flow is simpler.

The pump is a centrifugal type and so produces a pressure rise and flow rate linearly proportional to its speed. Figure 15 is the calibration plot of flow rate and jet velocity as a function of pump speed for three different slice thicknesses; it shows the common operating ranges for the apparatus. The data from this plot is provided in Appendix A. The velocity is calculated by dividing the flow rate by the cross-sectional area of the slice. These values were obtained using water in the flow system and measuring the time taken to drain a specific mass of water from the reservoir. To

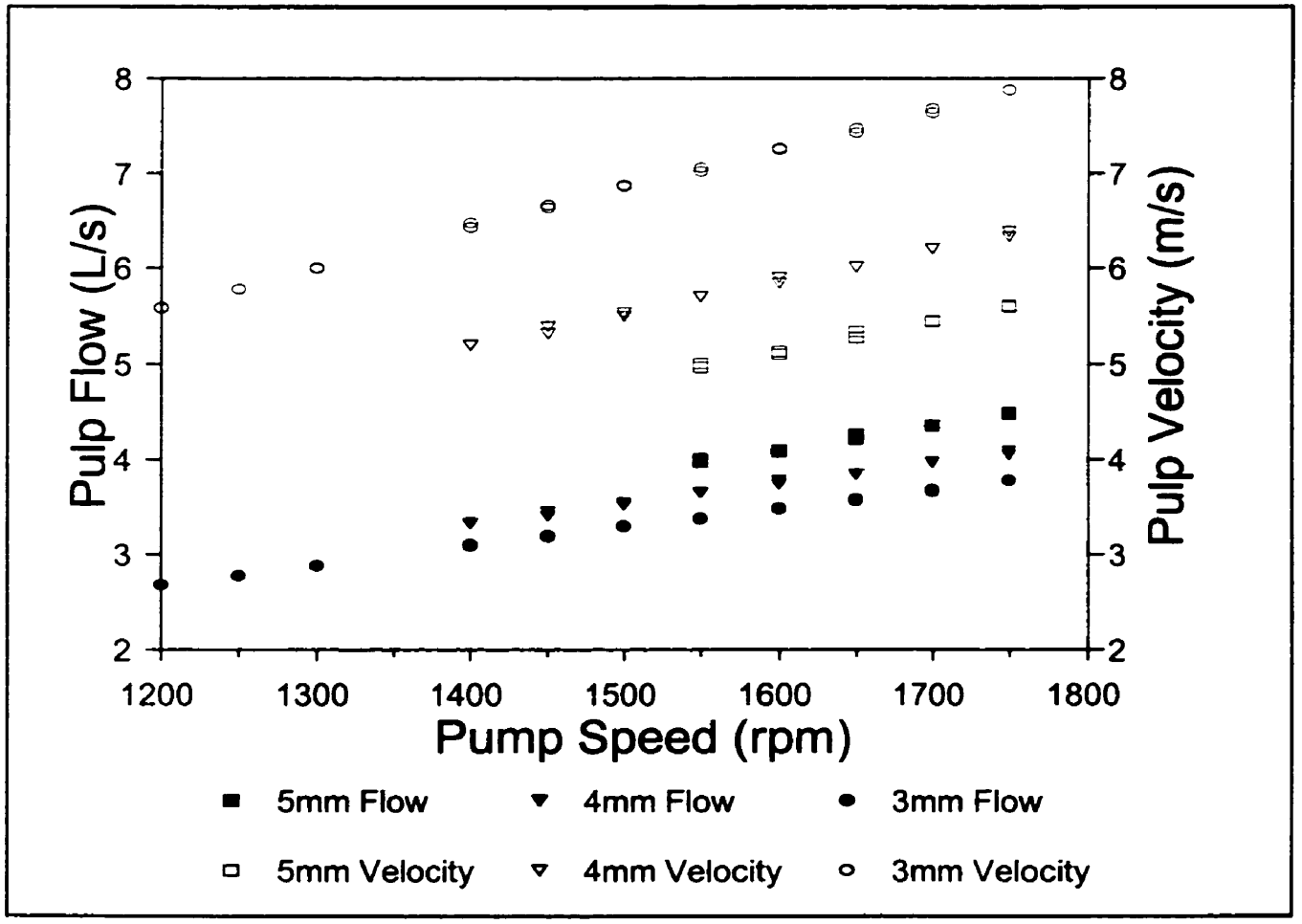

Figure 15: Plot of headbox flow rate versus pump speed

determine whether the height of water in the reservoir affected the flow rate, measurements were separately taken of the time to drain the first half of the reservoir contents and the second half. No difference was detectable (see Appendix A). A repeat of this calibration a few months later showed a decrease in pump performance. This was eventually found to be due to accumulated fibres blocking the openings in the distributor block, thus increasing the flow resistance. After that, cleaning of the headbox became a regular procedure.

It can be seen from Figure 15 that the flow rate decreases significantly with decreasing slice thickness, as the slice provides the largest resistance in the flow system (the distributor is the other large resistance). However, it can also be seen that jet velocity increases with decreasing slice

thickness. Even with a constant pump speed, the flow rate doesn't scale directly with slice thickness because the other resistances in the flow circuit remain constant. Mathematically, this idea is expressed as:

$$\dot{V} \propto \frac{\text{Pump Speed}}{\frac{1}{\text{Slice Thickness}} + \text{Other Resistances}} \qquad \text{(Eq. 3.3.1)}$$

Therefore, the relationship between flow rate and slice thickness is non-linear. Fluid velocity is proportional to the ratio between flow rate and slice thickness. As the slice thickness decreases, the ratio between the flow rate and the slice thickness increases, resulting in the higher fluid velocities (and thus the stronger dependance on pump speed) shown in Figure 15.

The slice thickness is set using spacers, so it can only be set to discreet intervals (those shown in Figure 15 are among them); consequently, the flow rate and jet velocity cannot be selected independently. If one specific parameter (either flow rate or velocity) is desired, then a slice thickness whose range includes that value must be chosen and the pump set to the correct speed. The other parameter is then necessarily set. However, different slice thicknesses will result in different values for the second parameter; the slice thickness giving the best value for the second parameter can be chosen.

3.4. Drainage Section

A schematic of the drainage section is shown in Figure 16. There are four general drainage zones in the machine: the jet impingement point, the forming roll, the blade section and the vacuum boxes. Each successive zone needs to remove considerably less water than the previous ones, but it must remove water that is shielded by an ever growing sheet structure. For example, at the

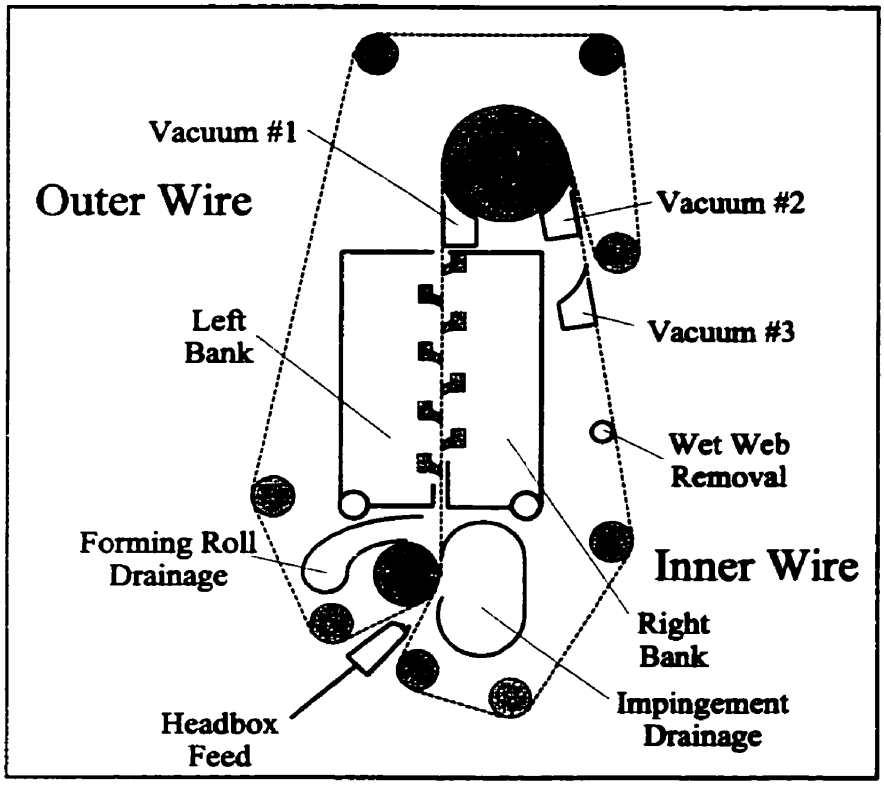

Figure 16: Schematic of the drainage section

impingement point, two thirds of all the water present will simply flow right through the wires, carried by the momentum of the jet; with no sheet yet formed, only the fabric resistance blocks the flow of water. At the other extreme, the final vacuum box withdraws very little water, but it must draw that water through a dense layer of fibres. Cellulose fibres can absorb many times their own mass in water into their solid structure; a "suspension" of only 10% solids is, itself, actually quite solid and will have very little water pooling at the low points. Industrially, pulp consistencies in the headbox are generally in the 0.1% to 1.0% range, and the wet sheet leaves the forming section in the range of 15% to 20% consistency.

The wires currently in use on the drainage section are of a design intended for the manufacture of newsprint and are made by Johnson Wires International. The machine-direction fibres are polyester woven at 146 strands per inch and the cross-direction fibres are a blend of polyester and nylon woven at 124.5 fibres per inch. Polyester is used as the base material because it is the easiest to weave and it provides excellent runnability on paper machines; nylon is added for its strength in order to provide abrasion resistance[28]. The wires are approximately 20 cm in width. The outer wire is 4.350m in length and the inner wire is 3.346m in length; under tension, they have

an initial extension of 0.06% and an elastic modulus of 1.31 MN/m. As these dimensions are very unusual and it was important that there be no seam, the wires had to be hand woven specifically for us.

Forming Roll Zone

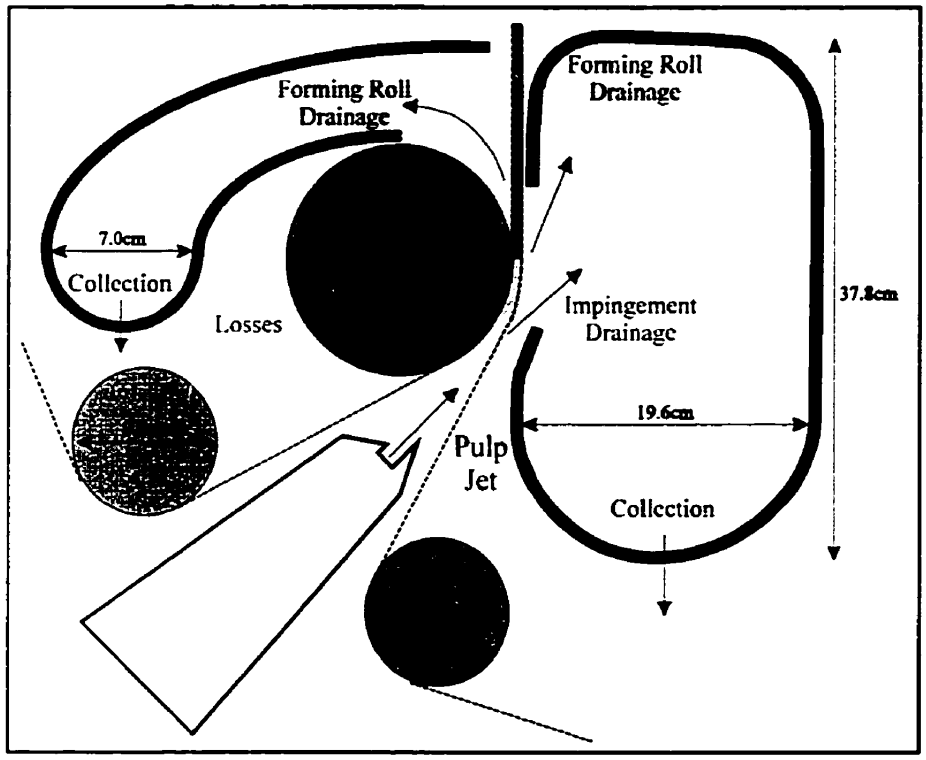

Figure 17: Schematic of the forming roll section

A close up schematic of the jet impingement and forming roll zone is shown in Figure 17. There are two important mechanisms of dewatering in this zone: impingement drainage and roll drainage. Impingement drainage occurs when the jet strikes the permeable wires; the momentum of the jet emerging from the headbox is sufficient to cause more than half the water in the pulp to pass through the wires at this point. This water will also carry with it a small fraction of the fibres. All this white water is collected in a large chamber (shown in Figure 17).

We can apply the Bernoulli equation to get an estimate of the drainage pressure the jet conveys as it strikes the inner wire. Assuming no frictional losses, we can write the equation from the slice of the headbox (h) to the point where the jet strikes the wire (w):

$$\frac{P_h}{\rho} + \frac{v_h^2}{2} + gz_h = \frac{P_w}{\rho} + \frac{v_w^2}{2} + gz_w \qquad \text{(Eq. 3.4.1)}$$

We can assume that P_h is equal to atmospheric pressure and drop that term, defining P_w as a gauge pressure. Referring to Figure 15, we see that velocities around 6 m/s are typical for a slice opening of 4mm. We can define $z_h = 0$ and set z_w to the height of the impingement point above the slice, approximately 6 cm. Finally, we can set $v_w = 0$. With these assumptions and rearranging, we obtain:

$$P_w = \rho(v_h^2 / 2 - gz_w) \qquad \text{(Eq.3.4.2)}$$

Taking the density of pulp to be that of water (1000 kg/m^3), we obtain a theoretical maximum drainage pressure of 17 kPa.

The remaining material is caught between the two converging wires and squeezed as they wrap around the forming roll. The tension in the wires (approximately 3000 N/m in the outer wire and 1200 N/m in the inner wire - Section 3.6) exerts sufficient pressure to drive more water from the pulp. As illustrated in Figure 17, water which migrates through the outer wire is mostly thrown off the wires by centrifugal force and collected in the same chamber as the white water from the impingement drainage.

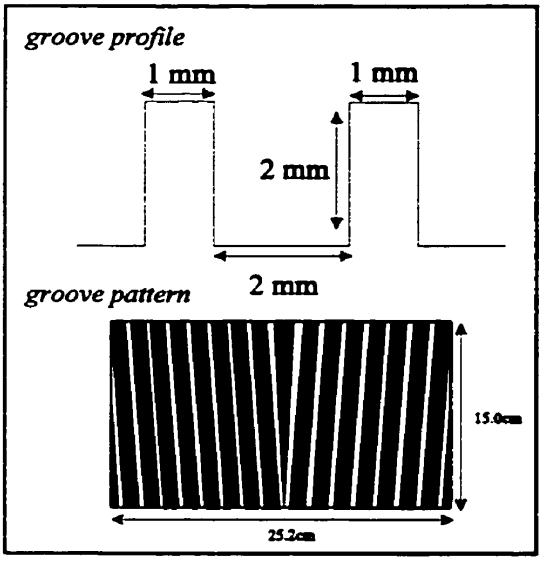

Figure 18: Forming roll profiles

The surface of the forming roll has a grooved structure, as illustrated in Figure 18. The grooves provide a space for the white water to seep into as the pulp is squeezed by the wires around the forming roll. The white water is then carried around and thrown out of the grooves

by centrifugal force. It is intercepted and collected in another chamber (Figure 17). The grooves start in the centre of the roll and spiral outward rather than forming one continuous groove all the way along; this was done to prevent them from "nudging" the wires in the direction of the spiral.

Estimation of the maximum drainage pressure exerted by wires wrapping around the forming roll is often made with the expression P = T/r, where P is the drainage pressure, T is the tension in the outside wire and r is the radius of the forming roll. This expression results from a simplified force balance around the forming roll. Figure 19 shows the general free body diagram for any roll with a wire wrapping around it. F_1 and F_2 are the forces exerted by the wires and F_r is the reaction force exerted by the roll. Since the roll is not accelerating, we can compose two force balances for the system:

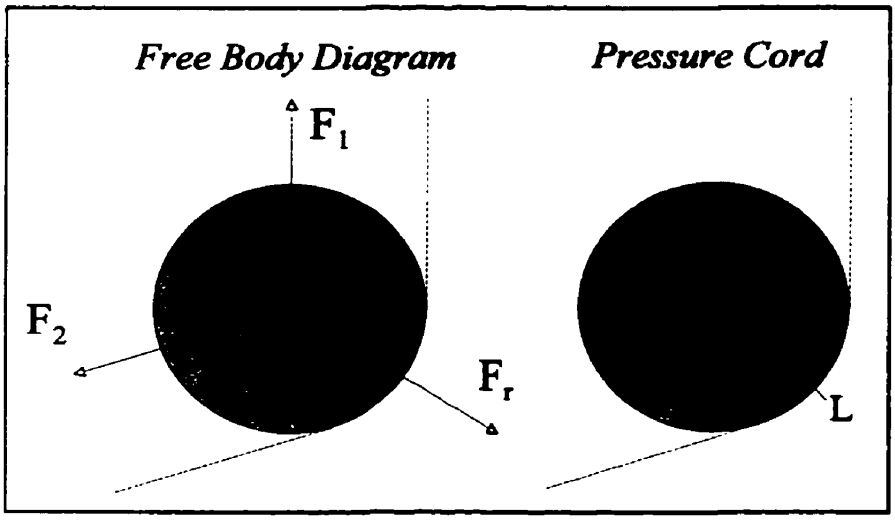

Figure 19: Free body diagram for a roll

$$F_1 + F_2 \cos\theta_2 + F_r \cos\theta_r = 0 \qquad \text{(Eq. 3.4.3)}$$

$$F_2 \sin\theta_2 + F_r \sin\theta_r = 0 \qquad \text{(Eq. 3.4.4)}$$

We can assume that both F_1 and F_2 are equal to F_w, the force of tension in the wire (this assumption is only correct in a static situation - if the wire is moving, the forces will have slightly different values), yielding:

$$F_w (1 + \cos\theta_2) + F_r \cos\theta_r = 0 \qquad \text{(Eq. 3.4.5)}$$

$$F_w \sin\theta_2 + F_r \sin\theta_r = 0 \qquad \text{(Eq. 3.4.6)}$$

which can be manipulated to give:

$$\theta_r = \tfrac{1}{2}\,\theta_2 \qquad \text{(Eq. 3.4.7)}$$

$$F_r = -2\,F_w \cos(\tfrac{1}{2}\,\theta_2) \qquad \text{(Eq. 3.4.8)}$$

Equation 3.4.7 is intuitively obvious, as the three vectors form a bilateral triangle. Equation 3.4.8 is logical, as F_r varies from 0 to 2 F_w as θ_2 varies from 180° to 360° (the range of possible angles). If we then draw a cord across the angle subtended by the tangent points of the two wires, we have the line designated L in Figure 19. The line L is essentially the one-dimensional "projection" of the wrap arc that the wire makes as it passes around the roll. Knowing the wrap angle, θ_L, and the roll radius, r, using the law of sines an expression for L can be derived:

$$L = r\,[\,2\,(1-\cos\theta_L)]^{1/2} \qquad \text{(Eq. 3.4.9)}$$

We can define the average pressure exerted on the roll surface by the wire as the roll reaction force, F_r, divided by the product of the cord length, L, and the roll width, W:

$$P = \frac{F_r}{L \cdot W} \qquad \text{(Eq. 3.4.10)}$$

or,

$$P = \frac{-2F_w \cos(\frac{1}{2}\theta_2)}{r[2(1-\cos\theta_L)]^{1/2} W} \qquad \text{(Eq. 3.4.11)}$$

Wire tension, T, is defined as the force in the wire, F_w, divided by the wire width, W. We can also recognize that $\theta_L = \theta_2 - \pi$. Therefore, we arrive at:

$$P = \frac{T}{r}\,\frac{-2\cos(\frac{1}{2}\theta_2)}{[2(1-\cos(\theta_2-\pi))]^{1/2}} \qquad \text{(Eq. 3.4.12)}$$

By using trigonometric definitions, it can be shown that the second fraction on the right hand side of Equation 3.4.12 is equal to unity; therefore, the equation reduces to P = T/r. Given the assumption

that the force acts across the flat projection L rather than the curved surface of the roll allows us to assume a uniform pressure profile with the value T/r. Around a real roll, the pressure profile will have a maximum at the middle of the arc and fall off to zero at the edges of the arc; the average pressure will be somewhat less than the value T/r, as the total surface area is larger for the arc than for the projection. However, the value T/r still gives us a reasonable estimate of the average pressure encountered by the pulp as it is wrapped around the roll.

It is this relationship, P = T/r, which requires that our machine inner wire tension be significantly lower than the machine outer wire tension, in order to compensate for our forming roll being very much smaller than that on an industrial machine. The inner wire of the machine (which is the OUTSIDE wire around the forming roll and thus controls the nip pressure) has a tension of approximately 2000 N/m, and the forming roll has a radius of 7.62cm, which results in a theoretical pressure peak of approximately 26 kPa. Industrial machines are generally in the range of 5 kPa. We are significantly higher because the wire tension has not been scaled down to the same extent as the roll radius.

Most of the removed water is collected in the impingement drainage chamber. The lower half of this chamber extends forward as a large spout which continuously drains the collected water into a plastic tank; this tank is manually graduated to measure how much water it contains. The forming roll collection chamber is drained by a rubber hose into smaller tank; this tank is weighed to measure its contents. It is also important to note that not all the white water is collected. As indicated in Figure 17, a small fraction of the drained water is lost around the lips of both collection chambers. Much of the water which is lost from the impingement chamber is instead captured by the right blade chamber. Water lost around the forming roll is mostly recirculated back into the wires and pulp jet.

Blade Zone

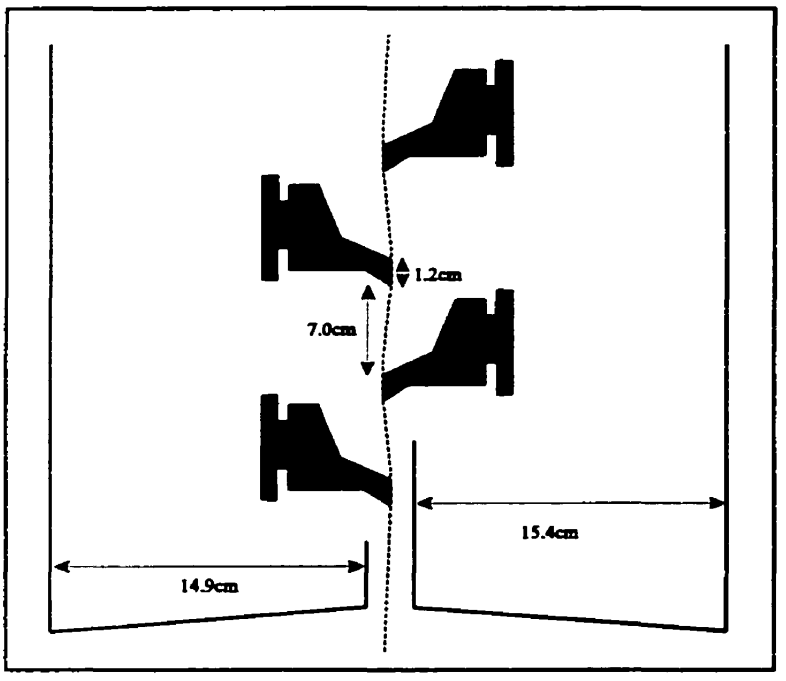

Figure 20: Schematic of the blade section

A close up schematic of part of the blade drainage section is shown in Figure 20. A series of nine staggered blades remove water from the pulp as the wires wrap lightly around the blades. Each blade also serves to scrape off the water driven out by the previous blade. All the water that is removed by the blades collects in the two blade chambers and is continuously drained out through a rubber tube into two separate tanks.

The blades used are a standard design for newsprint machines. They are made of low density polyethylene. Their T-shaped mounting structure in back is a standard European design. Each blade is mounted on a steel brace with the corresponding T-shaped mount. Any other blade using this configuration can be mounted on our brace. The braces are anchored directly into the frame of the apparatus. The holes in the brace that the anchors pass through are slotted, so that the brace can be moved horizontally. This allows us to control the degree of wire wrap around each blade. The pressure generated by the blade is proportional to the angle at which the wire approaches and wraps around the blade (Equations 2.1.4. and 2.1.5). It is necessary to increase slightly the wrap angle for each successive blade in order to increase the pressure spike it generates, as the remaining water for each successive blade will be harder and harder to remove. No attempt has yet been made to

optimize the blade configurations. The approaching and departing angles of all the blades currently range from 0° to 5°, with an average of around 2°.

The expression derived by Green allows us to estimate the magnitude of the pressure profile of a blade integrated over the entire length of the blade. This expression is:

$$\int p(s)\, ds = T \bullet \alpha \qquad \text{(Eq.3.4.13)}$$

where $\int p(s)\, ds$ is the integral of the pressure profile over the entire length of the blade, T is the tension in the outside wire going over the blade, and α is the sum of the approach and departure angles of the wires going over the blade (given in radians). Unfortunately, this model is simply a force balance and does not account for the effect of wire speed on the pressure profile.

For the outer wire, the tension is approximately 2400 N/m, and the wrap angle of our blades is approximately 2° (approaching and departing), for a total wrap of 4° = 0.07 rad. This gives an integrated pressure pulse of approximately 170 N/m. For our blades of 1.2 cm in height, this gives an average pressure of 14 kPa on the right bank of blades. The inner wire has a tension of only 2000 N/m, so the pressure spike generated by the left bank of blades will be approximately 12 kPa.

There has been no effort yet made towards optimizing the blade section. The ramifications of this will be discussed in the next chapter.

In addition to dewatering, the sharp pressure profile generated by the blades also serves to break up flocs and redisperse fibres. These flocs begin to form as water is removed and the fibres become more concentrated. The steep pressure spike results in small scale flow of water and fibres down the pressure gradient[29]. If the average fibre displacement that takes place is of the same length as the distance between flocs (on the order of a few millimetres), then this flow will "smooth out" the flocs. Without this effect, excessive flocculation would occur before drainage is complete,

leading to a sheet with a very grainy, irregular appearance. This effect can only be studied once our apparatus is capable of producing an intact sheet.

Vacuum Box Zone

Vacuum boxes provide the greatest driving force for water removal, which is why they are placed at the end of the drainage section. A sketch of the first vacuum box is shown in Figure 21; the others are similar. The vacuum to each box is provided by a 3 horsepower Shop-Vac heavy-duty vacuum cleaner (designed for wet pick up). Collection of the white water takes place in the body of the vacuum cleaners. Suction takes place at the narrow opening in the box which is in contact

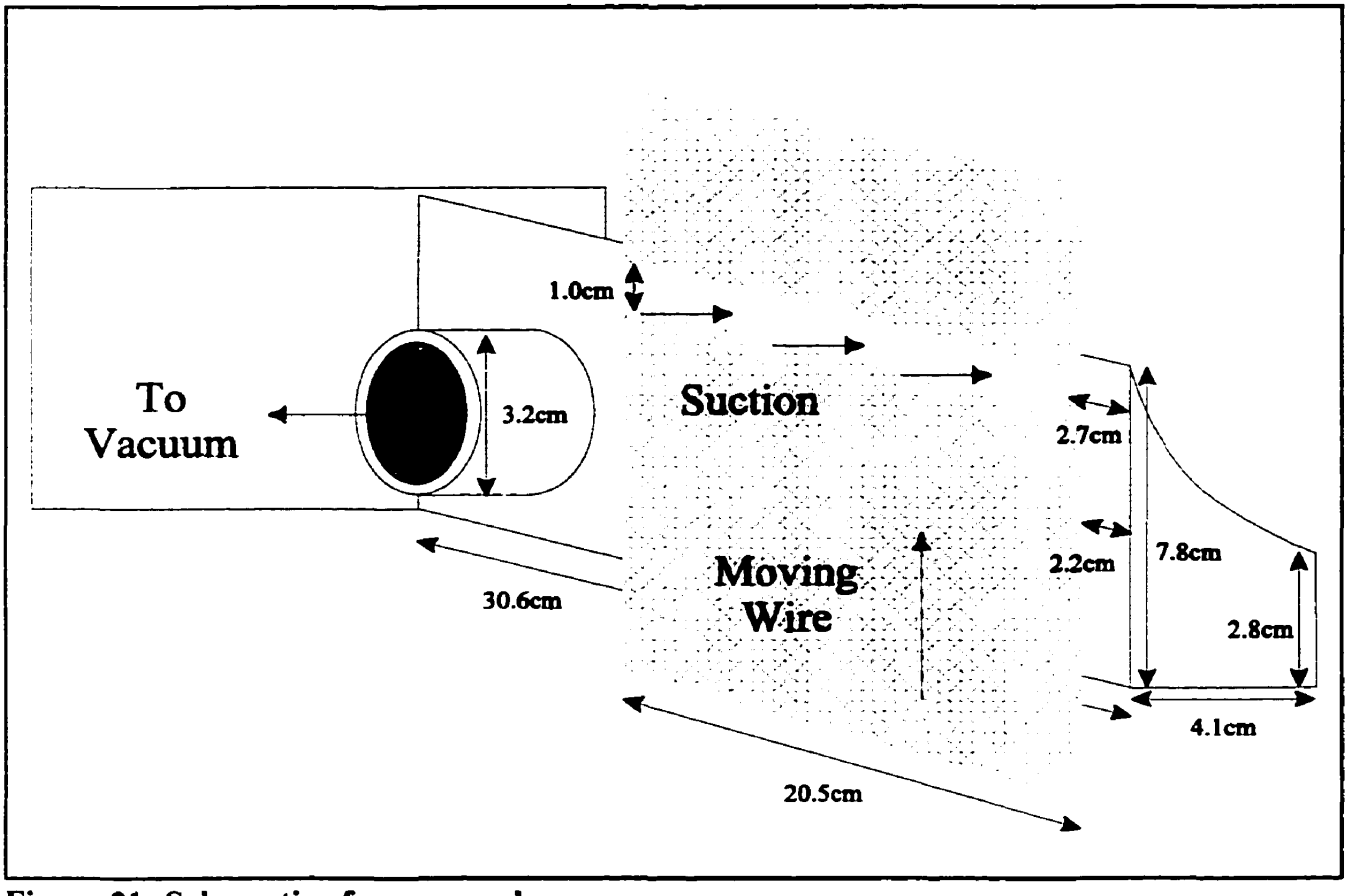

Figure 21: Schematic of a vacuum box

with the wires. Increasing the height of the gap would increase the time that the pulp is exposed to vacuum, but would increase the flow rate of air and thus decrease the level of vacuum. A larger gap would be appropriate for the first vacuum box, where the web is still thinner and so water is still more easily removed. However, no attempt has yet been made to optimize the size of the gaps; they are all currently one centimetre in height. Optimization of the vacuum boxes will be part of the future work on this project.

On a system with zero flow (a pressure gauge plugged into the end of the hose), the Shop-Vacs which power our vacuum boxes can generate a pressure of approximately 20 kPa below atmospheric pressure. The wires and web are permeable and allow a certain amount of air to flow through and entrain water. Therefore, the vacuum pulse generated by the boxes during operation will have a magnitude somewhat lower than 20 kPa. Industrial vacuum boxes are usually in the range of 10 kPa to 60 kPa, so we are still in the low end of industrial operation.

3.5. Pickup Section

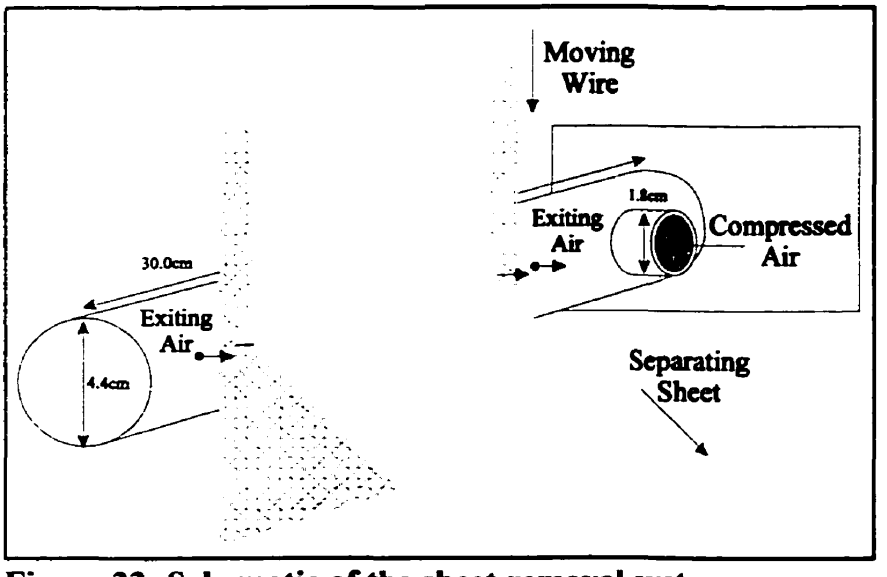

Figure 22: Schematic of the sheet removal system

The system for picking up the wet sheet is still under design. Currently, a pipe with a series of small perforations fed with compressed air is used to blow the sheet off the wires after the final vacuum box (Figure 22). The sheet is destroyed in the process

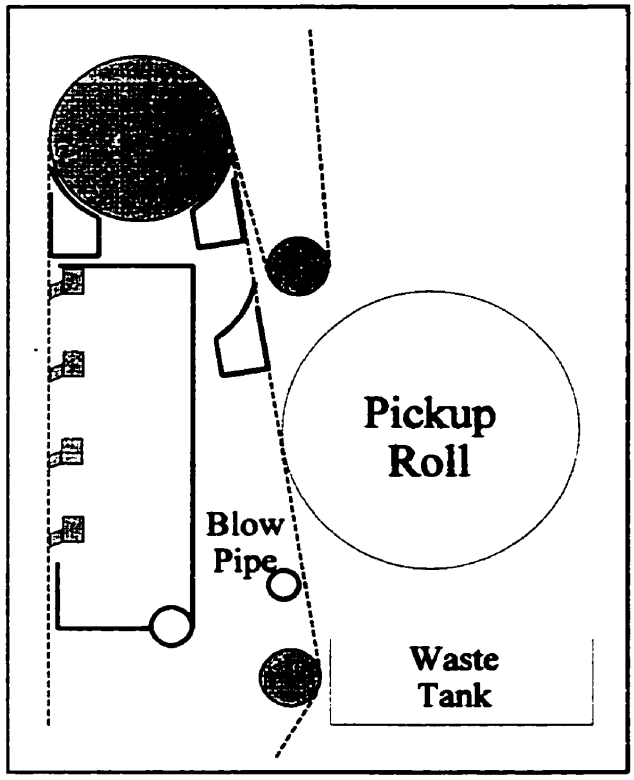

Figure 23: Schematic of the future sheet collector

but the material is collected in a plastic tank for analysis.

A schematic of the ultimate collection system is shown in Figure 23. It consists of a large roll which turns in contact with the inner wire after the final vacuum box. The roll is driven by the same motor which drives the wires to ensure synchronicity. As the sheet emerges from the drainage section, it contacts the roll and adheres preferentially to it by capillary action. A smooth, high surface energy material such as polished metal will be used to. After one complete revolution of the pickup roll, the sheet will be contacting the already collected wet sheet, which will not provide as good a grip. Therefore, the blowpipe will be retained at a lower position in order to blow off any sheet which is not collected on the pickup roll; it is also possible that a vacuum may be applied to the interior of the roll. All that is needed is for all the fibre to be collected by one of the two systems and for the pickup roll to acquire a solid, intact length of sheet. With these, a mass balance can be performed and the sheet structure can be analysed.

3.6. Subsystems

There are several secondary systems that are necessary for the apparatus to run correctly, such as the motive system, the wire tension system, and the wire guidance system. Each of these subsystems is shown in Figure 24 and is discussed below.

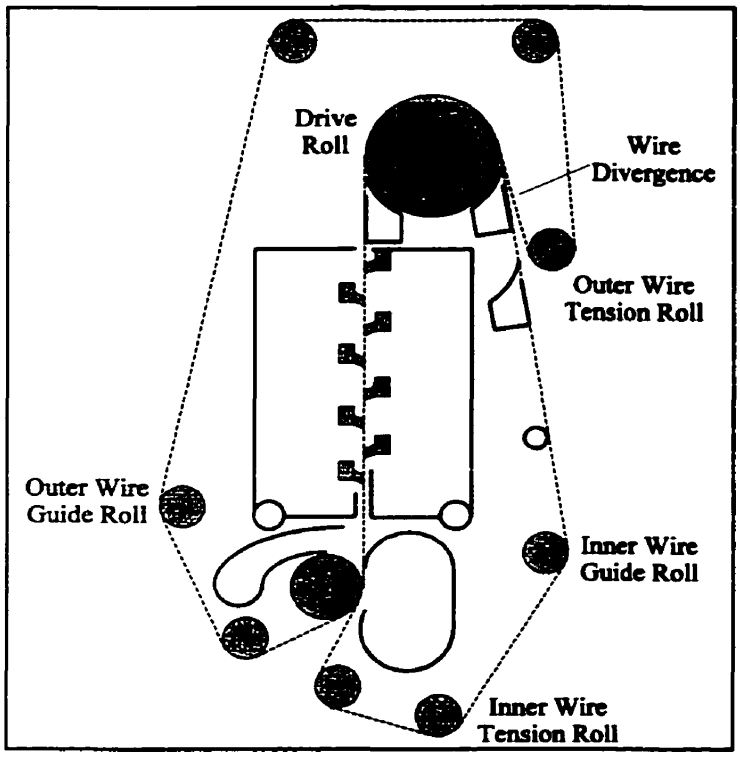

Figure 24: Schematic of the subsystems

System Assembly

All the components of the drainage section are connected onto a backing plate made of aluminum, three quarters of an inch thick. The plate is mounted on a broad-based steel frame which is bolted to the ground in the laboratory. The rolls and blades are put under stress by the tension in the wires, so they are mounted on large brackets which are, in turn, bolted onto the aluminum plate. The plate is sufficiently thick and supported that the tension in the wires does not cause it to bend during operation.

Motive System

The wires for the drainage section are driven by one roll; this is the large roll near the top of the machine between the first two vacuum boxes (Figure 24). It was decided to use just one roll in order to avoid the difficulty of synchronizing two rolls (much the same way the pickup roll will also be driven by this very same motor). A 3 horsepower motor drives the roll at a maximum speed of 1750 motor revolutions per minute; the motor is mounted on the steel frame of the system assembly. The gear system is currently set up for a maximum wire speed of approximately 5.3 m/s. However, this maximum could be modified upwards in the future. Cutting edge industrial machines can run in the range of 25 m/s to 50 m/s depending on the application, so increasing our operating range in the future will be an important task.

In the motor speed range of 1200 rpm to 1250 rpm, the motive system generates a harmonic vibration that causes the apparatus to shake disturbingly. The system is normally run well above this range and when accelerating the wires to operating speed, this speed range is passed through quickly.

The calibration plot showing wire speed as a function of motor speed is shown in Figure 25; the data from this plot are presented in Appendix A. Wire speeds were calculated by measuring the time for them to make either ten or twenty revolutions, and dividing ten or twenty times the length of the wire by that time. All measurements were made while the wires were wet but without a pulp or water jet. Measurements were taken at two motor speeds with a jet of water being fired into the

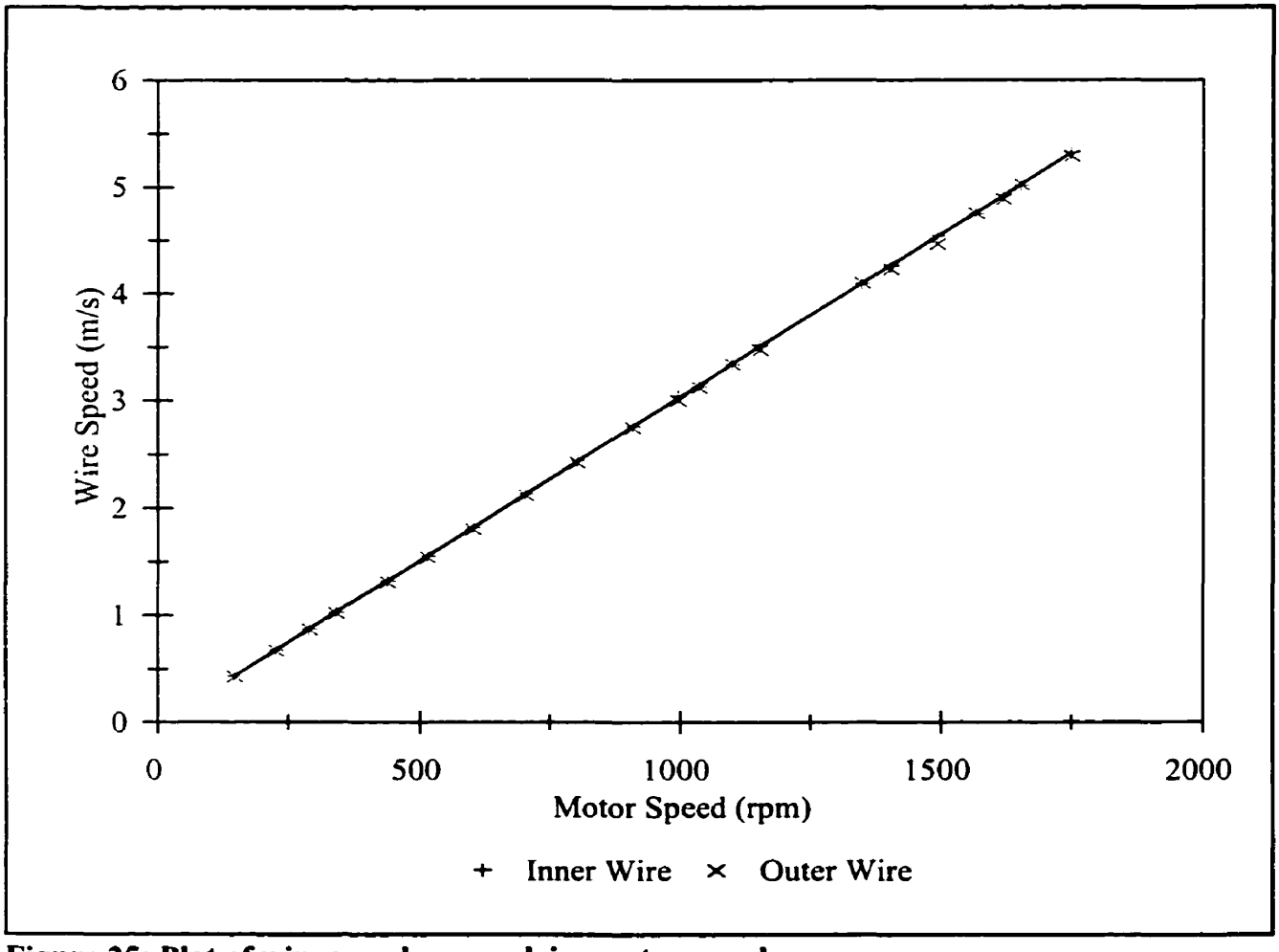

Figure 25: Plot of wire speed versus drive motor speed

machine, but it had no effect on the wire speeds. The outer wire has a length of 4.350m; the inner wire has a length of 3.346m. The two wires were found to have the same speeds, so no slipping occurs between the wires.

Wire Tension System

The tension in the wires is a very important system parameter. The outer wire requires a minimum tension in order to prevent it slipping against the inner wire at very high speeds. The tension in the inner wire is believed to affect how easily the pulp jet can penetrate between the wires; if the tension is too high, part of the pulp flow may not penetrate and can bounce back towards the headbox (this is called "backflow"). It also determines how strong the dewatering pressure around the roll will be. In the blade section, the tension of the far wire from any given blade determines how strong the dewatering pressure generated by that blade will be.

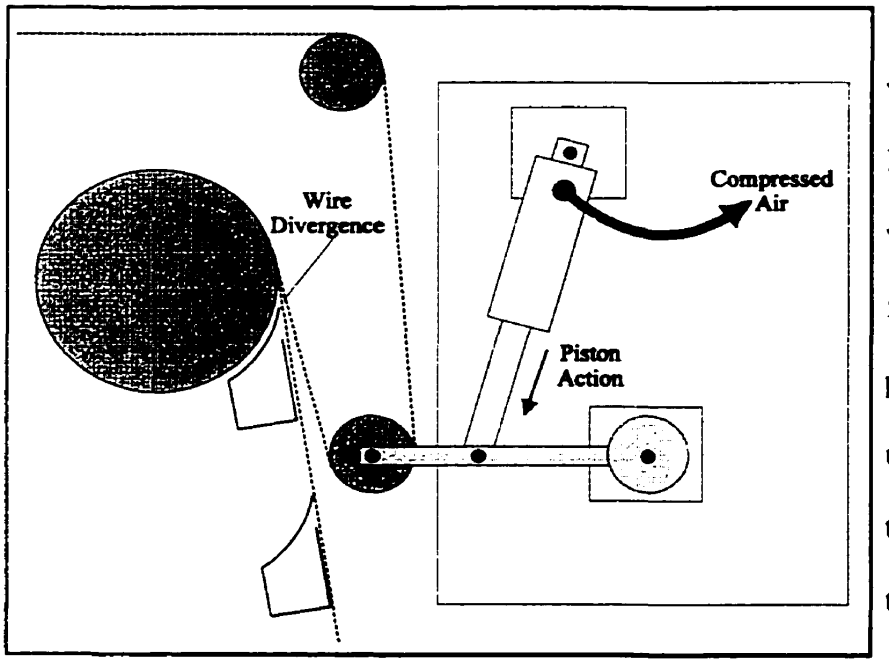

Figure 26: Schematic of the wire tension system

A schematic of the outer wire tension system is shown in Figure 26; the system for the inner wire is similar. Compressed air from a cylinder is fed into the piston. The piston exerts a force upon the arm which is suspending the roll. The force is, thus, transferred to the wire, which undergoes slight expansion.

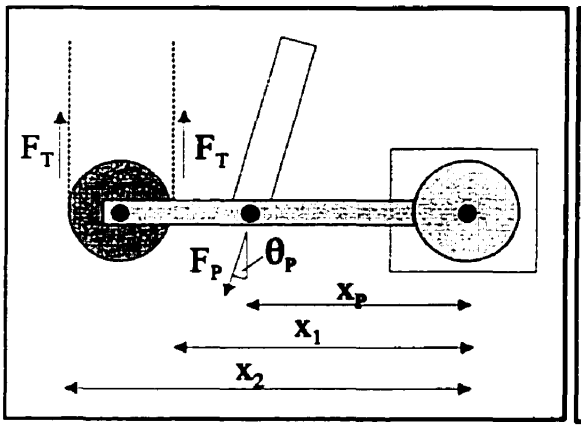

Figure 27: Free body diagram of the outer wire tension system

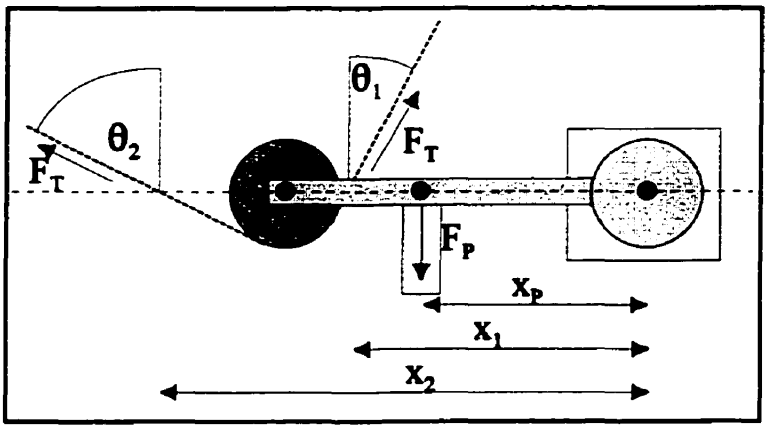

Figure 28: Free body diagram of the inner wire tension system

The tension in the wires can be calculated by performing a simple torque balance around each of the tension roll support arms. Free body diagrams for the outer wire arm and inner wire arm are shown in Figures 27 and 28, respectively. The notation is:

F_T = Force of tension in the wire
F_P = Force exerted by the piston
$\theta_{1,2,P}$ = Angle between the wire or piston and the normal
$x_{1,2,P}$ = Distance from centre of rotation to a force's point of action
τ_g = Torque exerted on the arm by gravity

τ_g was measured by a method of counterweights to be approximately 60 N·m.

The general expression of the torque balance for these systems is:

$$F_T \cos\theta_1 x_1 + F_T \cos\theta_2 x_2 + F_P \cos\theta_P x_P + \tau_g = 0 \qquad \text{(eq. 3.6.1)}$$

The piston force, F_P, is the product of the air pressure supplied to the piston, P_P, and the surface area inside the piston, A_P. The outer wire piston is supplied air behind the shaft, and has an internal chamber radius of 2.54cm; therefore, $A_P = 20.26\text{cm}^2$. The inner wire piston is supplied air before the shaft, which has an outer radius of 0.3125cm; therefore, $A_P = 18.28\text{cm}^2$. Also, the tension experienced by the wires, T, is defined as the force transmitted through the wires, F_T, divided by the width of the wires, 20.32cm.

For the outer wire, $\theta_2 = 6°$, $\theta_P = 15°$, $x_1 = 25.2cm$, $x_2 = 34.2cm$, $x_P = 21.8cm$. Substituting all these values into Equation 3.6.1 and rearranging gives an expression for outer wire tension (given in N/m) as a function of supplied air pressure (given in pascals):

$$T = 498.5\ N/m + (3.548 \times 10^{-3}\ m) \bullet P_P \qquad \text{(Eq. 3.6.2)}$$

Similarly for the inner wire, $\theta_1 = 20°$, $\theta_2 = 72°$, $x_1 = 25.2cm$, $x_2 = 40.0cm$, $x_P = 21.8cm$. Inserting these values into Equation 3.6.1 and rearranging gives an expression for inner wire tension (given in N/m) as a function of supplied air pressure (given in pascals):

$$T = 819.4\ N/m + (5.443 \times 10^{-3}\ m) \bullet P_P \qquad \text{(Eq. 3.6.3)}$$

Values of pressure normally used are 80psi = 550kPa for the outer wire, yielding a tension of 2400 N/m, and 30psi = 210kPa for the inner wire, yielding a tension of 2000 N/m.

The air line valves are rated to a maximum pressure of 150psi = 1000kPa. This would allow a maximum tension of 4000 N/m in the outer wire and 6300 N/m in the inner wire. Industrial machines generally run with wire tension in the range of 4000 N/m to 7000 N/m.

Point of Wire Divergence

The point at which the two wires separate occurs as they leave the drive roll, in the vicinity of the second vacuum box. This point also is illustrated in Figure 26. It is significant, because we require that the sheet remain attached to the inner wire when the two wires separate. Generally, when the wire separates from a roll there is a small vacuum generated in the gap where their surfaces come apart (the same phenomenon mentioned earlier with regards to the table rolls on Fourdrinier machines). This slight vacuum, assisted by the vacuum box immediately following, causes the wet sheet to remain upon the inner wire.

Wire Guidance System

With the very high speeds the wire section operates at, it is essential that the wires remain aligned and do not drift to either side as the paper is made. There is a guide roll for each wire, on either side of the machine. A schematic of the inner wire guide system is shown in Figure 29; the guide system for the outer wire is similar. One end of the axis on each of these guide rolls is adjustable so that it's orientation can be precisely controlled. By manipulating this, we are able to drive the wire in one direction or the other or have it remain motionless. The bracket which houses the adjustment system also has attached two metal plate barriers which constrain the movement of the wires; once the wires have been properly adjusted, these barriers can be positioned so as to prevent any drifting. The other rolls in the system are crowned to a slightly concave profile along their length; this also helps to keep the wires in a stable position.

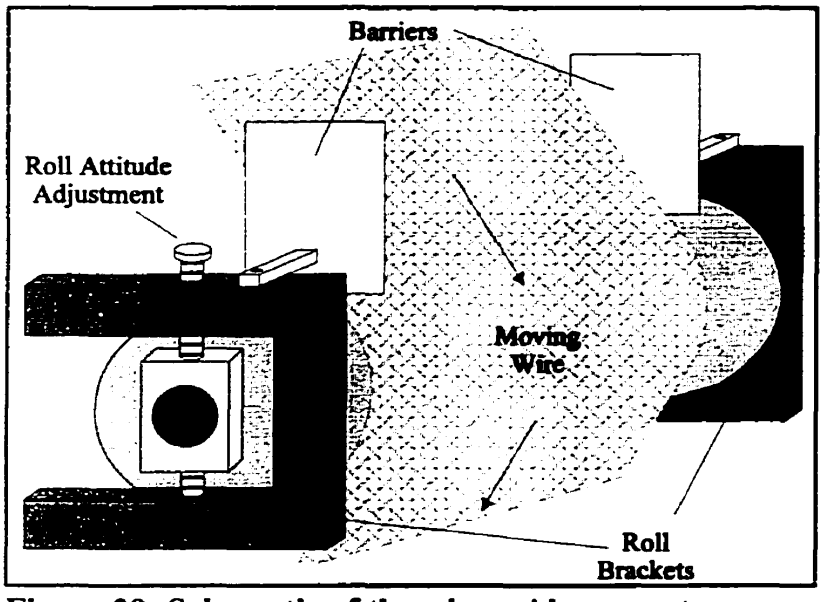

Figure 29: Schematic of the wire guidance system

Safety Systems

The entire apparatus is quite large and has many fast moving components. Put together, these constitute a potential for danger. Therefore, several safety features have been included in the system.

The control panel from which the entire system is operated is removed from the apparatus. After the initial preparation, all aspects of the machine operation can carried out from the control panel. The panel is directly wired into the motor controllers and the valve actuator. All the electrical connections to the control panel and all the connections from the motors and controllers to the power outlets are sealed and permanent; there are no plugs or wires which can accidentally become loose.

During operation, there is a mobile polycarbonate barrier which is put in place between the apparatus and the door to the lab. The barrier is 2.0m high and 0.9m wide to provide complete protection to people entering and exiting the lab.

Ear protectors or simple ear plugs are provided to all present in the lab while a run is going on. The drainage section makes considerable noise when in operation, and would be uncomfortable or damaging to those unprotected. Eye protection is also mandatory.

The system also has two "panic buttons" which immediately cut power to all systems when pressed. These buttons are large and red for easy visibility. One is on the control panel and the other is on the side of the drainage section away from the control panel.

3.7. System Operation

Before running an experiment, the operator must perform some advance preparations. The pulp in the reservoir must be prepared well ahead of time, to ensure complete dispersion and mixing of the fibres when the run begins. Also, each of the seven drainage points must be equipped with a tank or vacuum cleaner, the wires must be aligned and pre-wet, the pistons that put the wires under tension must be charged, and the air stream to remove the wet sheet must be activated.

To run an experiment, the operator simply powers up the pump and wires to their respective operating speeds. The valve in the headbox section is then switched and the pulp flow is diverted

to form the jet and is launched into the drainage section. Collection of drained water begins almost immediately at all seven points. Production of the sheet takes a few seconds longer, as the headbox line is usually filled with plain water. The reservoir is graduated, so that once a certain volume of pulp has been delivered, the valve is switched back to the recirculation line and both the drainage section and headbox section are slowed and shut down. The amount and composition of each white water stream is measured, as is that of the wet sheet.

The time required for the pulp jet to reach steady state has not been determined. Visually, it seems to form instantaneously, with no changes after the first second of operation. All experiments performed to date have assumed that an immediate steady state is achieved and that the end of operation is equally abrupt. A mass of 140 kg of pulp is delivered for all experiments. Such a large quantity is required both to increase the accuracy of the data and to reduce the significance of any transient effects at the beginning or end of the operation.

3.8. System Photographs

The following pages contain photographs of the apparatus.

The first is a photograph of the headbox section. Of particular interest is the piping arrangement that connects all the components together, and the arrangement of the mixers and the recirculation line in the reservoir. The headbox isn't actually shown, but the ridged plastic tube that leads to it is visible.

The second photograph is of the forming section. Of interest are the drainage ports on the collection chambers (which would normally have tubes connected) and the manner in which all the units are connected to the aluminum backplate. The top of the plate stands at a little over two metres in height. The headbox is also visible.

The third photograph shows the two systems together.

The fourth photograph is a close up of the headbox and forming roll section. The channel which drains the impingement chamber into a tank can be seen, as can the grooves on the forming roll.

The fifth photograph is a close up of the blade section. The blade mounts can be seen.

The sixth photograph is a close up of the vacuum section and drive roll. The second and third vacuum boxes do not have their hoses attached. The tension system for the outer wire is also visible.

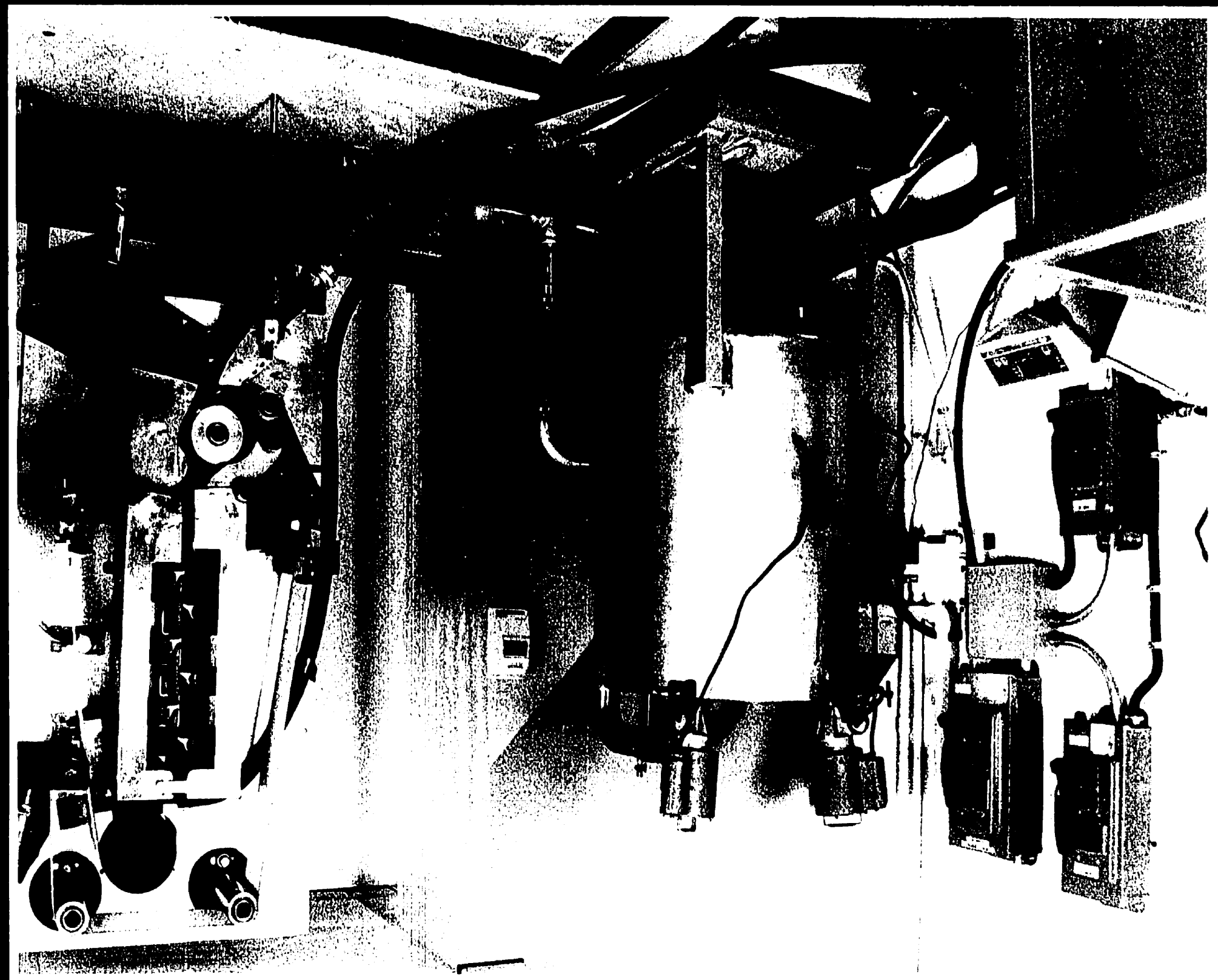

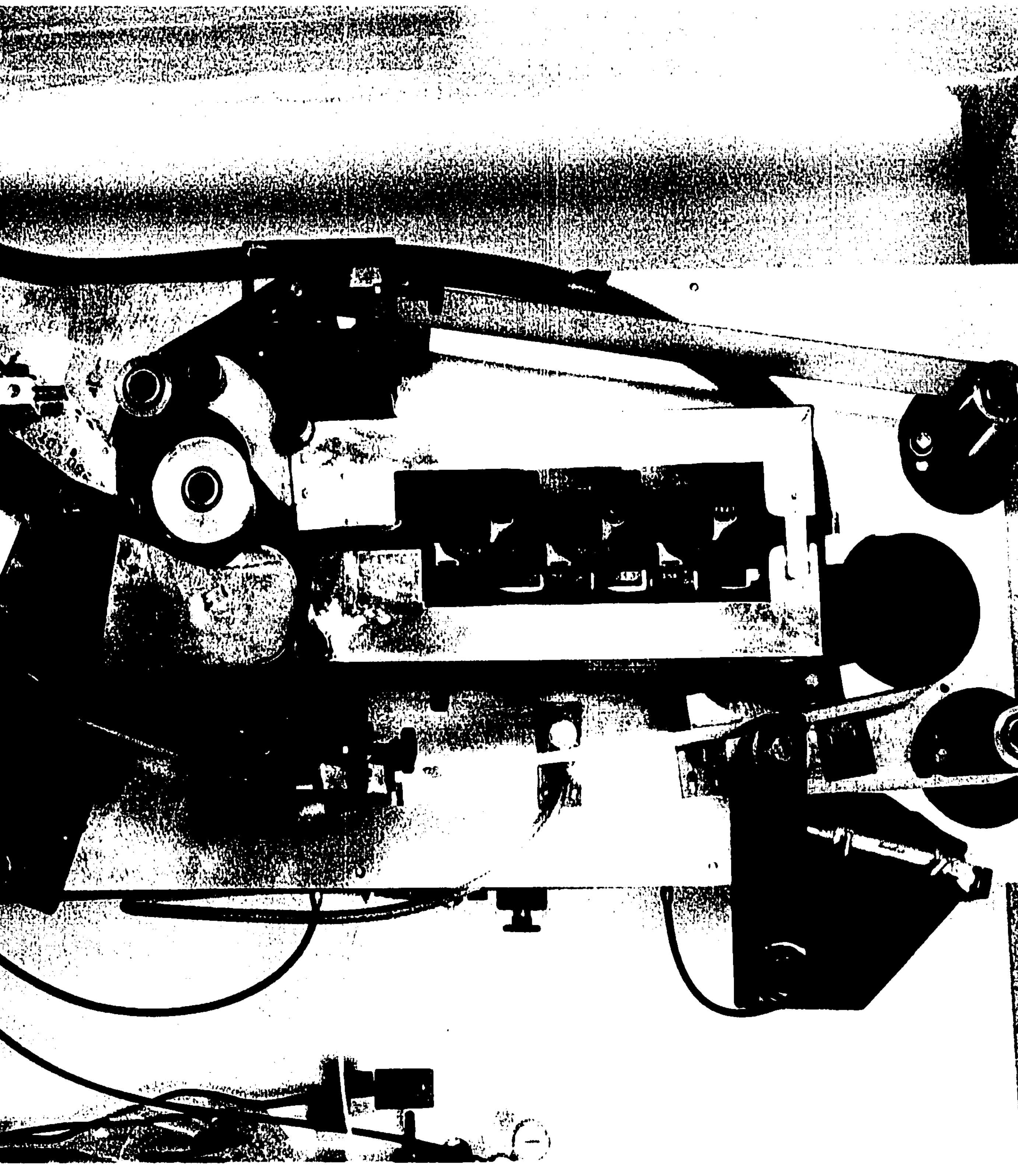

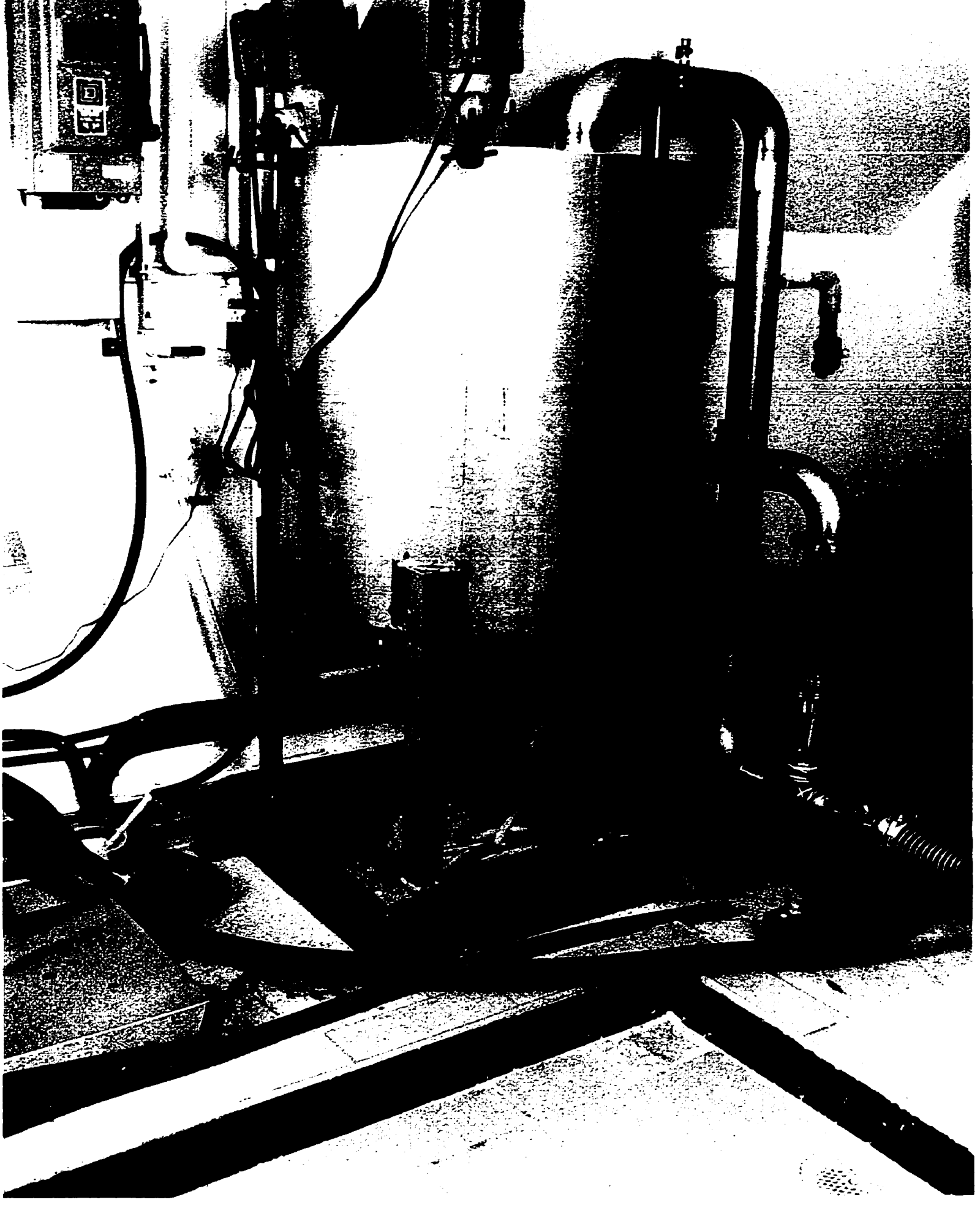

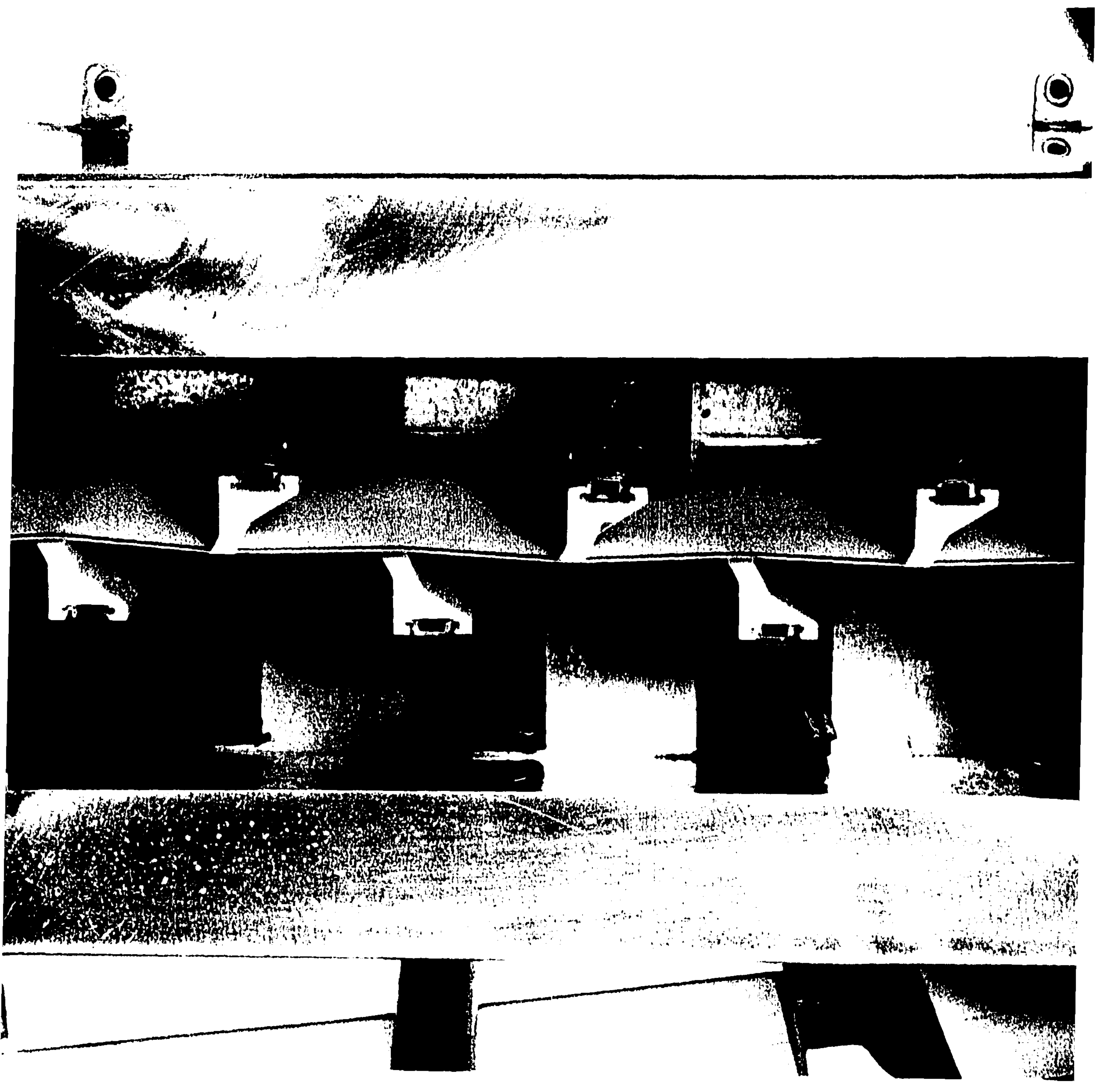

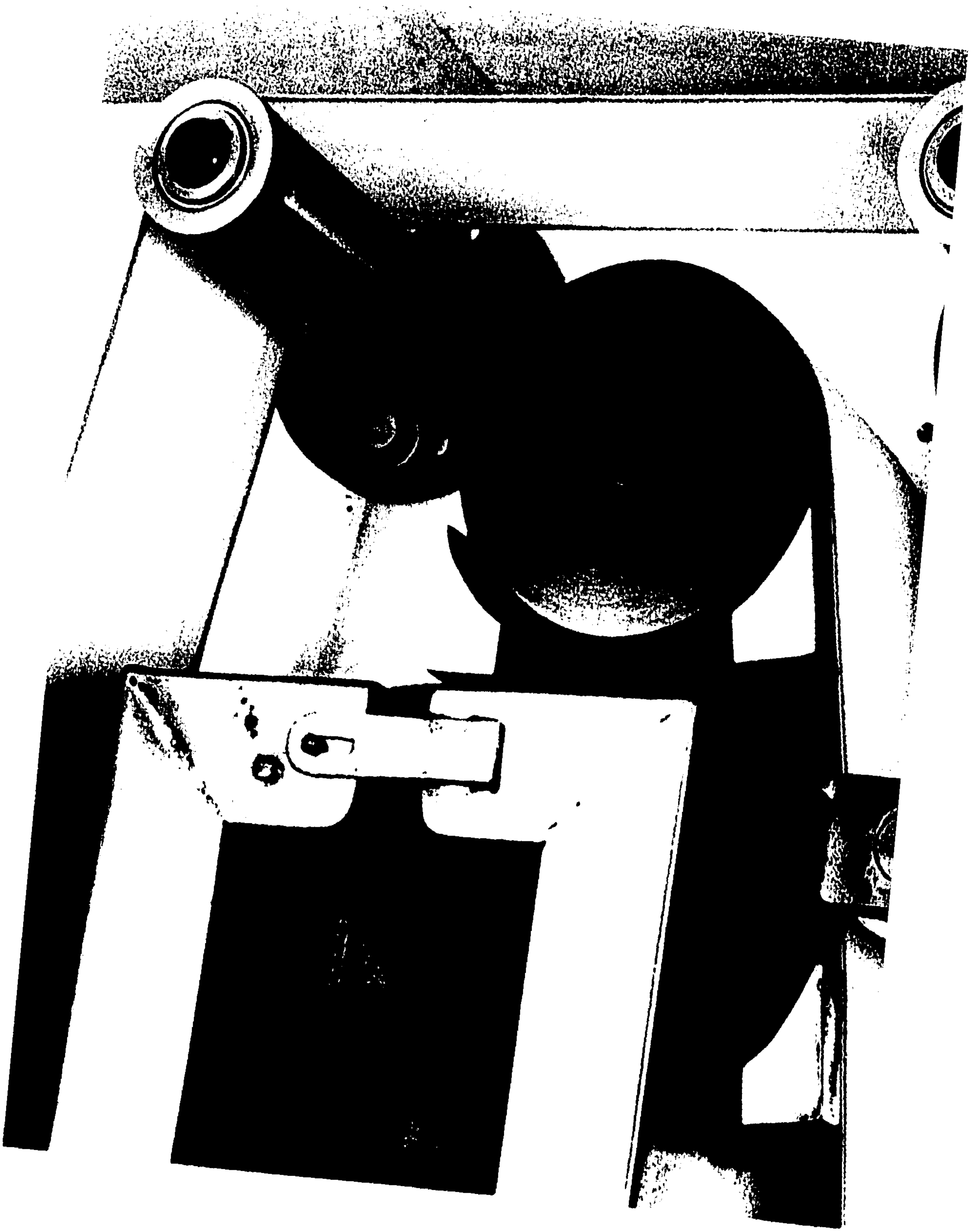

4. System Evaluation

The validation of this apparatus began with two preliminary concerns: first, that the data obtained from the apparatus is accurate and precise; and second, that the data and samples generated are actually useful. The first concern is simply a matter of system calibration and optimization and of refinement of the techniques used to carry out measurements. The second concern is more fundamental to the concept and design of the apparatus - essentially, can this apparatus fulfill our goal of simulating a broad range of papermaking conditions? Experiments were performed to address both concerns. The data obtained from the last five such experiments are presented in Appendix B, as are calculations performed with that data and explanations of how the calculations were carried out. Data from the fourth experiment is shown in Figure 30 and can be compared to that of an industrial machine shown in Figure 4. Many other experiments were performed; however, continued improvements in machine design and in measurement techniques over the last two years have rendered them obsolete.

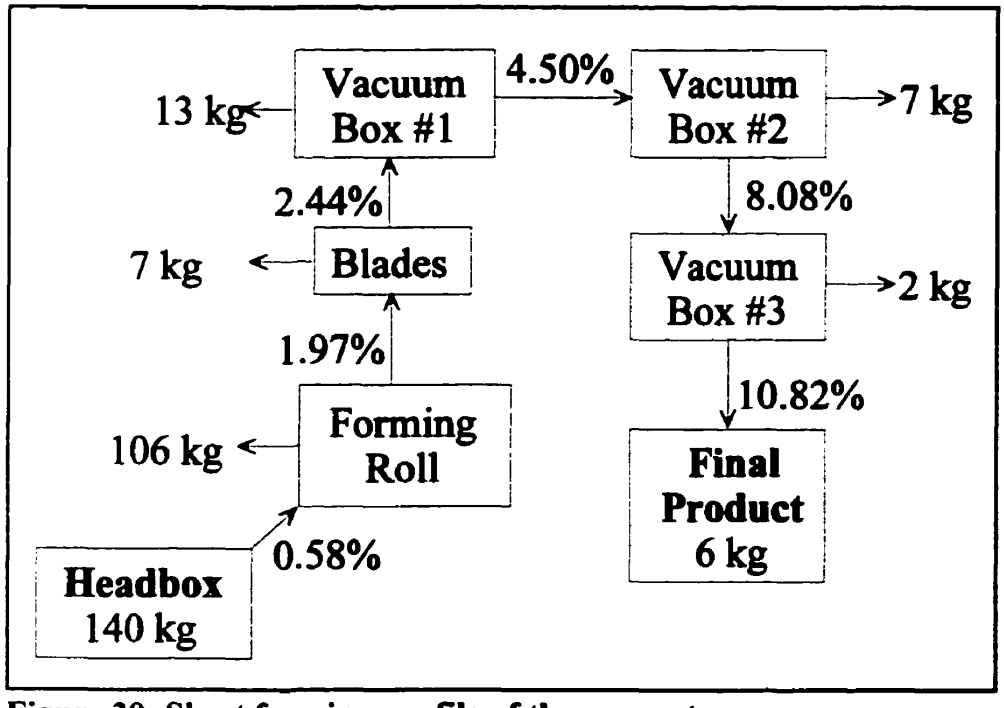

Figure 30: Sheet forming profile of the apparatus

4.1. System Accuracy

The first issue to be addressed was whether or not a complete mass balance could be closed around the system. With a total of one inlet stream and eight outlet streams, very high speeds and flow rates, a very open apparatus and a very compact design, there were initially a great many difficulties recovering even 80% of the material that was delivered. After many redesigns and modifications of various parts, we are now able to arrive at overall mass balances and fibre balances of better than 95%, and very often in the range of 98% to 99% (see data tables in Appendix B). In a few instances, the calculated mass balances exceed 100%, suggesting that the degree of error in our collection system is approaching the degree of error in the measurements of the stream mass and composition.

The most significant problem lay with the impingement drainage chamber. The initial design had a much smaller capacity and smaller exit spout. This resulted in the chamber constantly overflowing out the collection opening. Additionally, the geometry of the collection opening was such that water from the impingement point and from the forming roll was being excluded. All the difficulties arose from the simple fact that the chamber has to collect and divert an 8 L/s liquid stream coming in at 5 m/s. The stream has to be brought to a stop and deposited in a tank without losing any of the liquid and without capturing any other liquid from the system. The spatial constraints which had to be obeyed in designing the chamber were also quite limiting. Several redesigns were required before satisfactory operation was achieved.

Another significant problem is with the blowpipe sheet collection system. Although the system works, it is far from elegant. A small fraction of the fibre which is blown off the wires separates entirely from the sheet and sprays around the apparatus, becoming lost. Some of the fibre

is not even removed from the wire and usually ends up either on the floor or is thrown off the wire onto the underside of the headbox. The new roll pickup system should solve these difficulties.

The final significant problem we had was with the mixing in the reservoir of the headbox section. Initially, one small impeller was being used to mix the tank. As our ability to close the overall mass balance improved, the fibre balance began shooting up into the 120% range. Obviously, we could not be collecting more fibre than we were putting in, so the only possibility was that we were putting in more fibre than we thought. The next obvious conclusion was that the mixing in the reservoir was insufficient, causing a fibre concentration gradient to exist through the height of the tank. The pump was drawing pulp from the bottom of the reservoir to feed the headbox; samples for consistency measurement were being taken from the top, where the consistency was significantly lower. To solve this, a second mixer was added to the reservoir and larger impellers were acquired.

The actual measurement of the various streams has also been a significant problem. Until recently, all the white water streams were quantified using manually graduated volumetric tanks. The purchase of a large weighing scale improved these measurements incalculably. However, the white water from the impingement drainage chamber is collected in a 200L plastic tank which exceeds the capacity of the scale. The tank was, therefore, graduated in increments of 10kg of water; it is assumed that white water has the same density as plain tap water. Unfortunately, this arrangement allows estimates only to the nearest kilogram, whereas the scale reads to hundredths of a kilogram. The reservoir in the headbox section is similarly calibrated; recent recalibration of the reservoir using the scale showed that we were only delivering 140kg of pulp per experiment, when crude calibrations by volume had shown 150kg being delivered. Recalibration of these two containers has played a significant part in improving the mass balances in our experiments.

Measurement of the consistency of all streams and of the final product has been done by a simple dry-weight technique. This has the unfortunate effect of also measuring dissolved and suspended solids other than the fibres. This includes material from the fibres (a few percent by mass) and material in the tap water. Experiments have been performed which show that the concentration of mass added in the tap water is one order of magnitude lower than even the most dilute of white water streams. There is additional difficulty in measuring the wet sheet that emerges from the machine, because it is in the consistency range in which it exists as two phases: blobs of semi-solid, saturated fibres and free water which pools at the bottom of the tank. Both white water, which is a homogeneous suspension, and a semi-solid wet sheet completely drained of free water are easier to measure, as a uniform sample is easily obtained. As it is, the blobs of fibre must be well mixed with the free water in order to measure the overall consistency. As can be seen from the tables in Appendix B, the spread in these measurements is from 1 to 2 percentage points, on readings of around 10% or 11%. Fortunately, the recent modifications to the apparatus have brought the final sheet to the very edge of the consistency range in which free water is still present.

4.2. System Performance

Industrial paper machines produce a wet sheet with a consistency in the range of 15% to 20%. Ideally, we would like to be able to accomplish this same feat. Ideally, we would also like to subject the sheet to the same conditions over the course of its formation as it would experience on an industrial paper machine. Although we cannot, at present, measure the conditions of shear and turbulence experienced by the sheet in our apparatus, we can estimate the pressure profile to which it is subject and measure the resultant dewatering profile. Matching these two profiles to those

produced on an industrial machine would be a sufficient first step towards properly simulating the process.

The best variable to track in order to determine the effectiveness of drainage is the sheet consistency. As consistency increases, water becomes more difficult to remove, but the amount of water that must be removed to get an incremental change in consistency decreases. This is best illustrated by the tables in Appendix B. In the experiment from June 16th, 1998, the forming roll drainage removed 33 kg of water, resulting in a consistency increase of two percentage points; the first vacuum box only removed 9 kg of water, but this was sufficient to increase the consistency by almost two and a half percentage points. This behaviour arises because of the definition of consistency as a ratio between the mass of fibre and the total mass of the pulp or sheet. Each successive drainage unit in the sheet forming section has a higher driving force for water removal, but the resistance to water removal is increasing even faster; therefore, the drainage rate from one unit to the next generally decreases. However, the amount of remaining water is also decreasing, so the change in consistency from one unit to the next should remain approximately constant.

Figure 31 shows the consistency profile of the machine for all five experiments; the experiments are ranked in increasing order of pulp consistency. The consistency values listed are those *leaving* each section. An interesting observation is that for *all* experiments performed, the final consistency attained was around 11%. This is true for pulp consistencies ranging from 0.3% to almost 1.2%. This suggests that the final consistency is limited by the magnitude of the driving force applied for drainage.

For all drainage points up to and including the first vacuum box, the five experiments retain the same ratios in their consistencies (ie. on the graph, the heights of the bars keep the same relative heights from one section to the next). This tells us that (approximately) the same amount of water

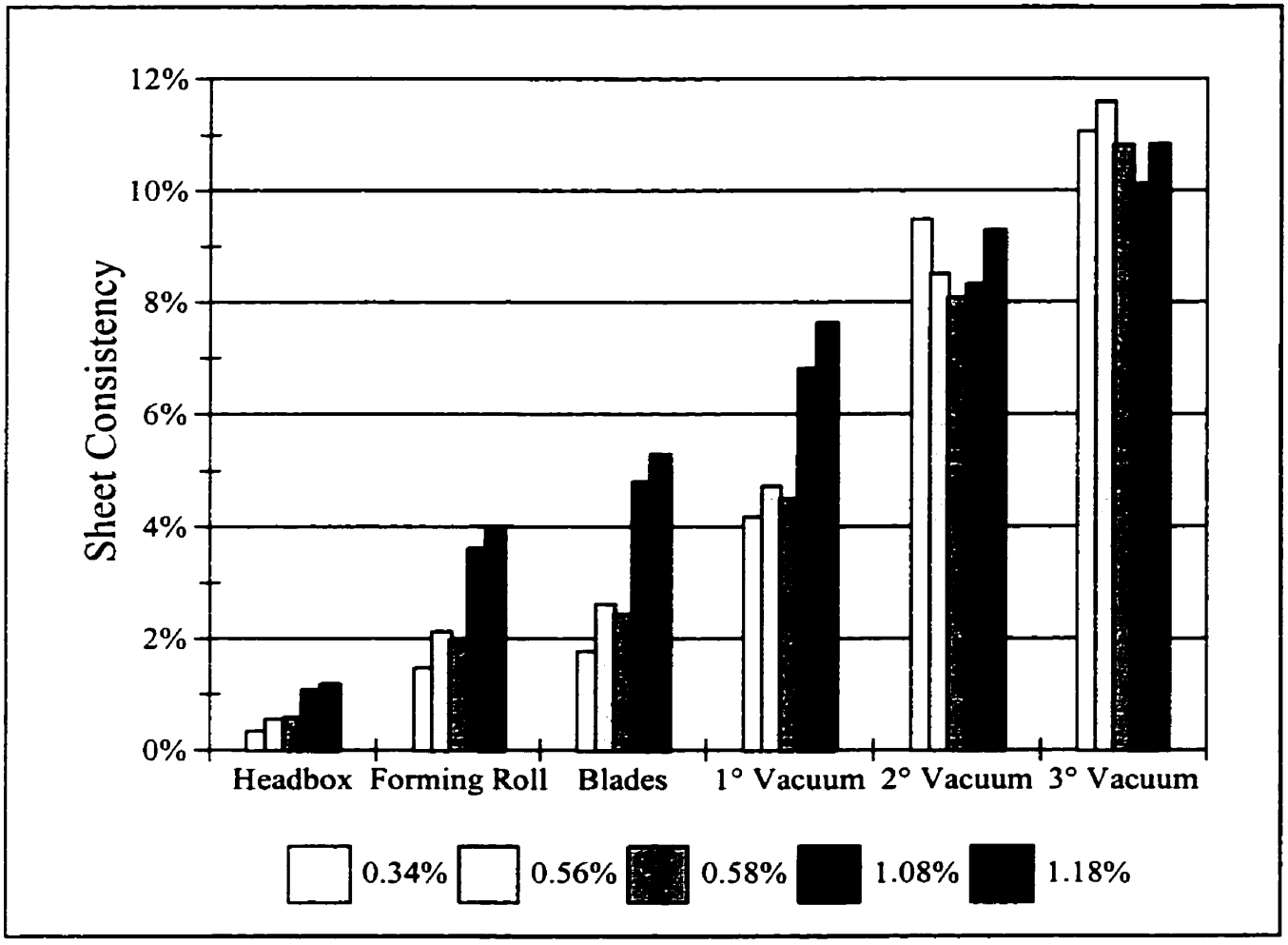

Figure 31: Consistency profile of the apparatus

is being withdrawn at these points for each run; this observation is confirmed in Figure 32, which plots the amount of water drained at each section. Only at the second and third vacuum boxes do the values of consistency even out, as the low consistency experiments catch up with the high consistency ones. At the forming roll and blades, and to some extent for the first vacuum box, the amount of water removed is only very weakly affected by the consistency of the initial pulp. This is because the pulp is still very dilute so this water is almost completely free of the fibres' influence. Therefore, it's removal is governed strictly by the geometry of the apparatus. Starting in the first vacuum box and then in the second one, the drainage rate decreases for the more concentrated pulps.

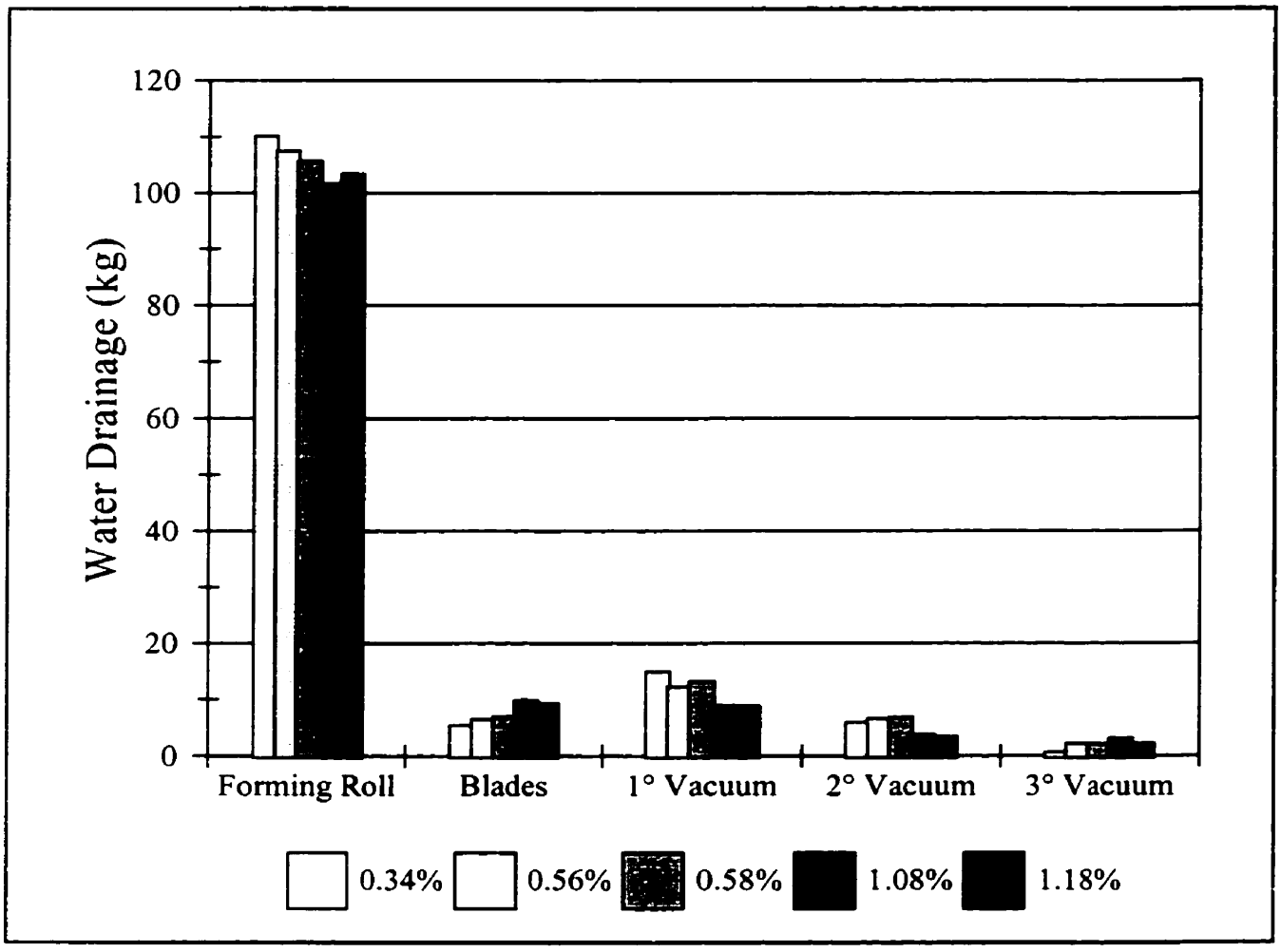

Figure 32: Drainage profile of the apparatus

This occurs because these higher consistency pulps reach sooner the consistency levels where the fibres start to impose a serious drainage resistance (8%-10%); after the second vacuum box, the low consistency pulps have also reached that level. By the third vacuum box, the drainage rate of all pulps has dropped off. They all have much the same sheet consistency, as they have all run into the same drainage barrier.

The limitation of the sheets to a consistency of 11% is due to the low dewatering forces at work. The forming roll and blades produce dewatering pressures in the 10 kPa to 15 kPa range; this is about double the industrial pressure for the forming roll, but about half that for the blades. The

vacuum boxes produce vacuums of around 20 kPa; industrial vacuum drainage starts at 20 kPa and increases up to 80 kPa vacuum in the couch roll. However, referring back to Figure 4, we see that industrial systems generally take the sheet to around 10% consistency between the vacuum section and the couch roll. This is precisely what our machine is doing. It is merely the lack of high-intensity vacuum at the end of the process that is currently limiting our drainage. Table 1 compares typical industrial drainage information with that obtained on our system. As can be seen, the overall effectiveness of the system is comparable to that achieved industrially; the vacuum that we impose on the sheet is producing the same results as comparable vacuums applied industrially. Higher vacuums in the second and third vacuum boxes will be necessary to obtain significantly higher sheet consistencies.

	Dewatering Pressure	Drainage (% of feed)	Leaving Consistency
	Industrial Conditions		
Headbox		100%	0.6%
Forming Roll	5-10 kPa	70%	2.0%
Blade Section	15-30 kPa	20%	6.0%
Vacuum Section	20-60 kPa	4%	10.0%
	Laboratory Conditions		
Headbox		100.00%	0.58%
Forming Roll	26 kPa	75.50%	1.97%
Blade Section	12-14 kPa	4.95%	2.44%
Vacuum Section	20 kPa	15.75%	10.82%

Table 1: Comparison of industrial conditions to laboratory conditions

In Table 1, the obvious weakness in the system is the blade section. Weak dewatering at the blades can also be seen in both Figures 31 and 32. In Figure 31, the low consistency pulps experience only a marginal increase in consistency going by the blades. This is because our blade section is producing the same driving force as the forming roll is; therefore, most of the water that the blades are capable of removing has already been removed at the forming roll. The vacuum section is then having to pick up the slack left by the inefficiency of the blades. Even for the high consistency pulps, the consistency increase at the blades is smaller than at the other sections. In Figure 32, the amount of water removed at the blade section is much lower than it should be; ideally, the amount of water removed should decrease smoothly from one section to the next. This problem arises because optimization of the blade section has not yet been performed. Once this is done, dewatering at the blade section will be much greater. The drainage profile in Figure 31 shows no signs of levelling off, so increasing the drainage at the blades should cause the entire profile to shift upwards a few percentage points. This will be the subject of future work.

4.3. Future Work

Apart from optimizing the blade section, several areas of operation still need to be explored:

The effect of the wire tensions on the drainage behaviour must be studied. Higher tensions should increase the pressure generated by the forming roll and the blades, but may hinder the flow of pulp into the nip where the wires converge.

The "freeness" of the pulp measures the degree of fibre bonding. A higher freeness value means that fibres bond together more strongly. However, this also makes it more difficult for water to escape and, hence, reduces drainage. The freeness is modified by beating the pulp. Altering the freeness of the pulp used should alter the drainage profile of the machine.

The transient periods of operation must also be studied. When the headbox jet is first formed, it takes a finite time to reach steady state operation. Long experimental runs are used now to minimize this effect, but shorter runs would be desirable to save time and fibre. Determining the nature and duration of the transient periods at both the beginning and end of an experiment will be an important part of the future work.

The web collection system is currently under construction. Once it is complete, it will be possible to collect sheet samples and dry them seperately in order to study the formation and other sheet properties. The first work will be to optimize the headbox design to deliver a uniform jet of pulp. Currently, there is no way to be certain that the velocity profile and consistency profile of the jet are uniform. Once this development has been made, then many more studies will become possible.

5. Conclusions

The world's first laboratory scale sheet former that simulates twin-wire roll-blade forming has been designed and developed. Its pressure profile can be manipulated to generate a wide array of conditions, including those typical of industrial papermaking. It has been refined to the point of being able to produce a paper web of 11% consistency from pulps of a broad range of consistencies. This is somewhat short of the 15% sheet consistency goal that is reached on industrial machines.

An overall mass balance around the system has been successfully closed to better than 95% and the fibre balance has been closed to similar levels.

The pressure profile of the machine has been estimated to reasonably simulate that of an industrial system. The resultant drainage has been shown to proceed gradually through the entire drainage section, as in an industrial machine. There are two exceptions to this: the blade section, which has not yet been optimized, generates small levels of dewatering in low consistency pulps; and the vacuum boxes, which exert only a low vacuum compared to the scale used in industry. Further work will be carried out to optimize these drainage units. Once this has been done, the entire drainage profile should approximately match that of an industrial machine and the goal of creating a 15% consistency sheet should be realized.

A system to acquire the wet sheet (or at least a sample thereof) is currently underway. Once this is completed, both a complete mass balance and a complete examination of the sheet structure will be possible. This will allow the simultaneous study of drainage, retention and formation in papermaking systems, something that has not before been possible.

To summarize, a twin-wire, lab scale sheet former has been constructed that allows study of drainage and retention in papermaking; therefore, the first objective of the project has been met.

Also, this former is able to produce a wet sheet of 11% consistency; because our goal was to generate a 15% consistency sheet, the second objective of the project has been partially filled. With further work, the second objective will be met completely.

6. References

[1] BAKER, D.E., RIEMER, K.N., "Twin-Wire Gap Forming: Leading Edge Technology for Newsprint in the 90s", *Pulp and Paper Canada*, 93(6):68-73 (1992)

[2] MANSON, D.W., "Pulp and Paper Manufacture, vol.7: Paper Machine Operations", ch.8: Fourdrinier Papermaking, p.192-215, *Canadian Pulp and Paper Association* (1991)

[3] THORP, B.A., "Pulp and Paper Manufacture, vol.7: Paper Machine Operations", ch.9: Principles of Twin-Wire and Multiple Wire Formation and Drainage, p.216-236, *Canadian Pulp and Paper Association* (1991)

[4] BIERMANN, C.J., "Essentials of Pulping and Papermaking", *Academic Press, Inc.*, Toronto (1993)

[5] ALLEN, L.H., YARASKAVITCH, I.M., "Effects of Retention and Drainage Aids on Paper Machine Drainage: A Review", Miscellaneous Report MR195, *Pulp and Paper Research Institute of Canada* (December 1990)

[6] BURKHARD, G., WRIST, P.E., "Investigation of High Speed Paper Machine Phenomena", *Pulp and Paper Magazine of Canada*, p.100-110 (March 1956)

[7] TAYLOR, G.I., "Drainage at a Table Roll", *Pulp and Paper Magazine of Canada*, Convention Issue, p.267-273 (1956)

[8] TAYLOR, G.I., "Drainage at a Table Roll and a Foil", *Pulp and Paper Magazine of Canada*, Convention Issue, p.172-176 (1958)

[9] GARNER, R.G., STONE, R.J., DAUNAIS, R., "A Simple Method of Estimating the Consistency of the Web in Twin Formers", PPR 702, *Pulp and Paper Research Institute of Canada* (October 1988)

[10] ZHAO, R.H., KEREKES, R.J., "Pressure Distribution Between Forming Fabrics in Blade Gap Formers: Thin Blades", *Journal of Pulp and Paper Science*, 21(3):J97-J103 (1995)

[11] ZAHRAI, S., BARK, F.H., NORMAN, B., "An Analysis of Blade Dewatering in a Twin-Wire Paper Machine", *Journal of Pulp and Paper Science*, 23(9):J452-J457 (1997)

[12] GREEN, S.I., "Analytical and Computational Modelling of Twin-Wire Blade Forming", *Journal of Pulp and Paper Science*, 23(7):J353-J357 (1997)

[13] GARNER, R.G., DAUNAIS, R., PYE, I.T., "Experimental Investigation of Drainage Around a Forming Roll", PPR 734, *Pulp and Paper Research Institute of Canada*, (March 1989)

[14] MARTINEZ, D.M., "Characterizing the Dewatering Rate in Roll Gap Formers", *Journal of Pulp and Paper Science*, 24(1):7-13 (1998)

[15] MEYER, H., "Hydrodynamics of the Sheet Forming Process", *Journal of the Technical Association of the Pulp and Paper Industry*, 54(9):1426-1450 (1971)

[16] KERSHAW, T., CUTSHALL, K.A., "The Current State of Drainage Theory", CPPA Technical Section Annual Meeting Conference Monograph, *Canadian Pulp and Paper Association Technical Section* (January 1978)

[17] PARKER, J.D., "The Sheet-Forming Process", *Technical Association of the Pulp and Paper Industry*, Atlanta, GA (1972)

[18] GAVELIN, G., "Paper Machine Design and Operation", *Angus Wilde Publications, Inc.*, Vancouver (1998)

[19] SCOTT, W.E., "Principles of Wet End Chemistry", *Technical Association of the Pulp and Paper Industry Press*, Atlanta (1996)

[20] "Forming Handsheets for Physical Test of Pulp", Canadian Pulp and Paper Association Standard Test Methods, Standard C.4 (1997)

[21] TAM DOO, P.A., KEREKES, R.J., PELTON, R.H., "Estimates of Maximum Hydrodynamic Shear Stresses on Fibre Surfaces in Paper Machine Wet End Flows and in Laboratory Drainage Testers", PPR424, *Pulp and Paper Research Institute of Canada*, (April 1983)

[22] SAURET, G., "Appareil de laboratoire permettant l'obtention de papiers anisotropes", *Association Technique pour l'Industrie Papetier*, 16(6):446-452 (1962)

[23] ANCZUROWSKI, E., JONES, A.Y., RUTLAND, D.F., "Simulation of fourdrinier paper machine forming in the laboratory", *Pulp and Paper Canada*, 84(12):T283-T286 (1983)

[24] SAURET, G., LONVERT, J., "Essais de reproduction de papiers industriels au laboratoire", *Techniques et Recherches Papetieres*, 4(8):80-91 (September 1966)

[25] SAURET, G., TRINH, H.I., "Etude de laboratoire sur la fabrication du carton", *Revue de l'Association Technique pour l'Industrie Papetiere*, 23(1):7-12 (1969)

[26] TREPANIER, R.J., "Dynamic Forming: Parameters for making oriented sheets in the laboratory", *Pulp and Paper Canada*, 90(4):45-48 (1989)

[27] MALASHENKO, A., "Theory and Practice of Papermaking: Headbox Operations", *Canadian Pulp and Paper Association* (1996)

[28] STOWE, B.A., EDGAR, C.B., ROOT, R.H., "Pulp and Paper Manufacture, vol.7: Paper Machine Operations", ch.22: Paper Machine Clothing, p.563-593, *Canadian Pulp and Paper Association* (1991)

[29] ZHAO, R.H., KEREKES, R.J., "The effect of consistency on pressure pulses in blade gap formers", Miscellaneous Report MR 316, *Pulp and Paper Research Institute of Canada* (1995)

Appendix A: Design Data

Pump Flow Rate Calibration Data

Table A.1 shows the data obtained to determine the effect of the liquid level in the reservoir on the flow rate of pulp generated by the pump. The difference in flow rate for the first half of the delivered pulp and the second half is calculated and the mean and standard deviation of the difference values is also calculated. The 95% confidence interval[1] about the mean can be calculated as

$$\mu_s \pm \frac{t_{\alpha/2} s}{n^{1/2}} \qquad \text{(Eq. A.1)}$$

where μ is the sample mean, s is the sample standard deviation, n is the number of degrees of freedom, and $t_{\alpha/2}$ is the critical 95% t-variate and is found from a table to be 2.228. Equation A.1 gives a confidence interval for the population mean, μ_p of

$$-0.02581 < \mu_p < 0.01141$$

Because this interval includes zero, it can be concluded that the difference in flow rates is equal to zero and, hence, there is no effect of liquid level height on flow rate.

---

[1]MASON, R.L., GUNST, R.F., HESS, J.L., "Statistical Design and Analysis of Experiments", *Wiley Interscience*, Toronto (1989)

Table A.1

Pump RPM	Time for 70L (s)	Time for 140L (s)	1st 70L Flow (L/s)	2nd 70L Flow (L/s)	Difference in Flow (L/s)
1750	16.66	33.29	4.20	4.21	-0.0076
1750	16.63	33.06	4.21	4.26	-0.0512
1750	16.73	33.31	4.18	4.22	-0.0379
1700	17.10	34.22	4.09	4.09	0.0048
1700	17.19	34.17	4.07	4.12	-0.0504
1650	17.55	35.09	3.99	3.99	-0.0023
1650	17.41	34.86	4.02	4.01	0.0092
1600	17.98	36.11	3.89	3.86	0.0322
1600	18.15	36.22	3.86	3.87	-0.0171
1550	18.55	37.24	3.77	3.75	0.0283
1550	18.50	37.06	3.78	3.77	0.0122
			Mean		-0.0072
			Standard Deviation		0.0277

Wire speed calibration data

Table A.2 presents the data in Figure 25, the plot of wire speed versus motor speed. At low speeds, the time taken to complete ten wire revolutions was measured; at high speeds, to maintain accuracy, twenty revolutions were taken. Knowing the length of the wires (4.350m for the outer wire and 3.346m for the inner wire), speeds were then calculated. Revolutions were counted by observing the passage of a coloured band on the wire. Measurements were taken while increasing the speed and while decreasing it, to check for hysteresis; none was apparent.

Table A.2

Motor RPM	TIME (s) Outer Wire 10 revs.	Outer Wire 20 revs.	Inner Wire 10 revs.	Inner Wire 20 revs.	SPEED (m/s) Outer Wire	Inner Wire
147	99.83		77.45		0.44	0.43
292	49.89		38.63		0.87	0.87
439	32.97		25.55		1.32	1.31
602	23.92		18.5		1.82	1.81
805	17.81		13.79		2.44	2.43
997	14.29		11.15		3.04	3.00
1102	13.02		10.02		3.34	3.34
1349		21.26		16.31	4.09	4.10
1492		19.16		14.98	4.54	4.47
1617		17.68		13.7	4.92	4.88
1750		16.34		12.64	5.32	5.29
1652		17.34		13.32	5.02	5.02
1565		18.32		14.08	4.75	4.75
1404		20.43		15.81	4.26	4.23
1155	12.36		9.63		3.52	3.47
1037	13.88		10.71		3.13	3.12
911	15.74		12.17		2.76	2.75
704	20.41		15.75		2.13	2.12
515	28.02		21.66		1.55	1.54
343	42.25		32.76		1.03	1.02
227	64.06		49.64		0.68	0.67
147	100.02		77.45		0.43	0.43

Appendix B: Experimental Data and Calculations

The data presented herein are in tabular format. Each table is a summary of an entire run with the apparatus. Each row is a sample taken from a given stream and each column is a collection of all like measurements or calculations. Here is a listing of all the columns and there meanings:

Stream refers to which stream the samples were taken from. Each of the white water streams has two replicates while the pulp and the wet sheet each have four replicates. "1° Forming" refers to the impingement drainage chamber, "2° Forming" refers to the forming roll drainage chamber, and "Left" and "Right Banks" refer to the chambers around the banks of blades.

Dish # refers to which of the twenty two labelled dishes the sample was put in.

Dish Mass is the mass of the sample dish.

With Pulp is the mass of the dish with the sample (not necessarily actual pulp).

With Dried Fibre is the mass of the dish and sample after being oven dried.

Mass of Pulp is the mass of the dish subtracted from the mass of the dish with the sample.

Mass of Fibre is the mass of the dish subtracted from the mass of the dish with dried sample.

Flow Consistency is the calculated solids fraction of the sample, taken by dividing the mass of fibre by the mass of pulp.

Bucket Mass is the mass of the container used to receive the stream in question. It is not listed for the pulp or primary forming roll because both have containers too large to weigh; these have, therefore, been manually graduated. This also means they have less accurate readings.

With Stream is the mass of the collected stream in its container.

Stream Mass is the mass of the container subtracted from the mass of the container with the stream.

Stream Consistency is simply the average of the values from the Flow Consistency column.

Stream Fibre is the total amount of fibre which exited the system through that stream; it is the stream mass multiplied by the stream consistency.

Remaining Fibre is the calculated amount of fibre that continued past that section through the sheet forming process, rather than having been drained out in a white water stream. It is the original amount of fibre minus all the previously washed out fibres.

Remaining Water is the calculated amount of water still left in the pulp after leaving that drainage section. It is the original amount of water minus all the water that has been removed up to that point.

Sheet Consistency is the calculated consistency of the sheet after leaving that drainage section. It is the remaining fibre divided by the sum of the remaining fibre and remaining water.

Total Collected is the total mass or total mass of fibre from all the outlet streams.

Recovery is the is the total collected divided by what was originally delivered, either for total mass of for fibres.

Losses is the difference between the total collected and what was originally delivered, either for total mass or for fibres. In the Sheet Progression columns, these values are added to the measured collected values of the secondary forming roll collection, in order to make the final sheet consistency match that which is measured. That stream was chosen because it has, by far, the most visible losses taking place during operation and so is the most likely source of losses.

The experimental data tables are listed in chronological order. It is important to note that as experiments they are not completely comparable with one another, as the pulp used in each run was not the same. The first experiment, carried out on June 15th 1998, used old pulp that had been used many times in previous experiments. During each successive use of a pulp, fines are selectively depleted. As mentioned in Chapter 2, fines play a significant role in impeding drainage; therefore, a pulp depleted of fines should drain more easily. The second experiment used a fresh batch of pulp; that same batch of pulp was then used for the third through fifth experiments. It is reasonable to assume that fines were gradually lost over the course of the experiments. However, given the small number of experiments carried out, it is impossible to determine for certain whether this had an effect on the drainage behaviour of the pulp. The pulp used for all these experiments was a bleached kraft pulp which typically has a very small fines fraction to begin with, so it is possible that fines depletion had a small effect or none at all. Since no gross change in the drainage behaviour occurred between experiments, it is assumed that there was no effect, and the experiments have been compared to one another for analytical purposes.

Flow Analysis

Stream	Dish #	Dish Mass (g)	With Pulp (g)	With Dried Fibre (g)	Mass of Pulp (g)	Mass of Fibre (g)	Flow Consistency	Mass Balance: Bucket Mass (kg)	Mass Balance: With Stream (kg)	Mass Balance: Stream Mass (kg)	Fibre Balance: Stream Consistency	Fibre Balance: Stream Fibre (kg)	Sheet Progression: Remaining Fibre (kg)	Sheet Progression: Remaining Water (kg)	Sheet Progression: Sheet Consistency
Headbox	0	1.862	51.471	2.031	49.609	0.169	0.34%			141	0.34%	0.4794	0.4794	140.52	0.34%
	1	1.853	48.966	2.020	47.113	0.167	0.35%								
	2	1.851	50.968	2.017	49.117	0.166	0.34%								
	3	1.868	57.237	2.049	55.369	0.181	0.33%								
1° Forming	4	1.024	28.048	1.032	27.024	0.008	0.03%			107	0.03%	0.0336	0.4458	33.55	1.31%
	5	1.012	19.133	1.018	18.121	0.006	0.03%								
2° Forming													0.4517	30.39	1.46%
Left Bank	6	1.018	15.633	1.025	14.615	0.007	0.05%	0.89	2.04	1.15	0.05%	0.0005	0.4511	29.24	1.52%
	7	1.017	13.753	1.023	12.736	0.006	0.05%								
Right Bank	8	1.025	19.369	1.035	18.344	0.010	0.05%	0.89	5.09	4.20	0.05%	0.0020	0.4491	25.04	1.76%
	9	1.015	24.279	1.025	23.264	0.010	0.04%								
Vacuum #1	10	1.007	19.132	1.018	18.125	0.011	0.06%	6.25	21.17	14.92	0.05%	0.0079	0.4411	10.13	4.17%
	11	1.009	27.226	1.021	26.217	0.012	0.05%								
Vacuum #2	12	1.005	19.936	1.013	18.931	0.008	0.04%	5.78	11.73	5.95	0.04%	0.0026	0.4386	4.18	9.49%
	13	1.022	19.203	1.030	18.181	0.008	0.04%								
Vacuum #3	14	1.027	22.343	1.036	21.316	0.009	0.04%	5.78	6.44	0.66	0.04%	0.0003	0.4383	3.52	11.07%
	15	1.031	20.292	1.040	19.261	0.009	0.05%								
Sheet	16	1.854	37.387	5.901	35.533	4.047	11.39%	4.06	8.02	3.96	11.07%	0.4383	Losses: (included in 2° f.roll)		
	17	1.850	44.619	6.566	42.769	4.716	11.03%						-0.0058	3.17	
	18	1.844	73.302	9.100	71.458	7.256	10.15%								
	19	1.861	42.205	6.581	40.344	4.720	11.70%								
								Total Collected (kg):		138		0.4852			
								Recovery:		97.8%		101.2%			

Date: June 15th, 1998

Outer Wire Pressure: 80psi
Inner Wire Pressure: 30psi
Slice Opening: 4mm
Pump Speed: 1750rpm
Wire Speed: 1750rpm

Notes: First run with 3° vacuum box
1° and 2° forming roll collectors lumped together
First run with 2° and 3° vacuum boxes siliconed

Machine Profile	Drainage	Cumul. Drainage	Remain. Water	Sheet Consistenc
Headbox	0.00	0.00	140.52	0.34%
Forming Roll	110.17	110.17	30.35	1.46%
Blades	5.35	115.52	25.00	1.76%
1° Vacuum	14.92	130.44	10.08	4.17%
2° Vacuum	5.95	136.39	4.13	9.49%
3° Vacuum	0.66	137.05	3.47	11.07%

Flow Analysis

Stream	Dish #	Dish Mass (g)	With Pulp (g)	With Dried Fibre (g)	Mass of Pulp (g)	Mass of Fibre (g)	Flow Consistency	Mass Balance: Bucket Mass (kg)	Mass Balance: With Stream (kg)	Mass Balance: Stream Mass (kg)	Fibre Balance: Stream Consistency	Fibre Balance: Stream Fibre (kg)	Sheet Progression: Remaining Fibre (kg)	Sheet Progression: Remaining Water (kg)	Sheet Progression: Sheet Consistency
Headbox	0	1.860	53.924	2.459	52.064	0.599	1.15%			141	1.18%	1.6612	1.6612	139.34	1.18%
	1	1.849	57.170	2.502	55.321	0.653	1.18%								
	2	1.846	54.516	2.474	52.670	0.628	1.19%								
	3	1.849	59.363	2.533	57.514	0.684	1.19%								
1° Forming	4	1.861	45.752	1.896	43.891	0.035	0.08%			60	0.09%	0.0514	1.6097	79.39	1.99%
	5	1.859	47.643	1.901	45.784	0.042	0.09%								
2° Forming	6	1.864	53.582	1.915	51.718	0.051	0.10%	2.11	35.20	33.09	0.10%	0.0318	1.4960	36.03	3.99%
	7	1.862	55.307	1.912	53.445	0.050	0.09%								
Left Bank	8	1.864	45.465	1.907	43.601	0.043	0.10%	0.89	3.89	3.00	0.10%	0.0030	1.4930	33.04	4.32%
	9	1.852	40.529	1.892	38.677	0.040	0.10%								
Right Bank	10	1.871	53.740	1.918	51.869	0.047	0.09%	0.89	7.27	6.38	0.09%	0.0056	1.4874	26.66	5.28%
	11	1.853	53.958	1.897	52.105	0.044	0.08%								
Vacuum #1	12	1.861	42.434	1.911	40.573	0.050	0.12%	6.25	15.05	8.80	0.12%	0.0107	1.4767	17.87	7.63%
	13	1.834	50.586	1.892	48.752	0.058	0.12%								
Vacuum #2	14	1.860	45.412	1.903	43.552	0.043	0.10%	5.78	9.29	3.51	0.10%	0.0034	1.4733	14.37	9.30%
	15	1.838	54.022	1.889	52.184	0.051	0.10%								
Vacuum #3	16	1.840	53.486	1.891	51.646	0.051	0.10%	5.78	8.05	2.27	0.10%	0.0022	1.4711	12.10	10.84%
	17	1.875	46.134	1.916	44.259	0.041	0.09%								
Sheet	18	1.862	65.811	8.896	63.949	7.034	11.00%	4.06	17.63	13.57	10.84%	1.4711	Losses: (included in 2° f.roll)		
	19	1.867	58.202	7.799	56.335	5.932	10.53%						0.0819	10.30	
	20	1.855	73.011	8.996	71.156	7.141	10.04%								
	21	1.849	127.630	16.690	125.781	14.841	11.80%								
								Total Collected (kg):		131		1.5793			
								Recovery:		92.6%		95.1%			

Date: June 16th, 1998

Outer Wire Pressure: 80psi
Inner Wire Pressure: 30psi
Slice Opening: 4mm
Pump Speed: 1750rpm
Wire Speed: 1750rpm

Machine Profile	Drainage	Cumul. Drainage	Remain. Water	Sheet Consistenc
Headbox	0.00	0.00	139.34	1.18%
Forming Roll	103.39	103.39	35.95	3.99%
Blades	9.38	112.77	26.57	5.28%
1° Vacuum	8.80	121.57	17.77	7.63%
2° Vacuum	3.51	125.08	14.26	9.30%
3° Vacuum	2.27	127.35	11.99	10.84%

Notes: The tank wasn't filled up to the mark when run, so less than 141kg was actually delivered
Used virgin bleached softwood kraft pulp

Flow Analysis

Stream	Dish #	Dish Mass (g)	With Pulp (g)	With Dried Fibre (g)	Mass of Pulp (g)	Mass of Fibre (g)	Flow Consistency	Mass Balance: Bucket Mass (kg)	Mass Balance: With Stream (kg)	Mass Balance: Stream Mass (kg)	Fibre Balance: Stream Consistency	Fibre Balance: Stream Fibre (kg)	Sheet Progression: Remaining Fibre (kg)	Sheet Progression: Remaining Water (kg)	Sheet Progression: Sheet Consistency
Headbox	0	1.849	44.662	2.303	42.813	0.454	1.06%			141	1.08%	1.5207	1.5207	139.48	1.08%
	1	1.854	51.724	2.389	49.870	0.535	1.07%								
	2	1.865	54.454	2.434	52.589	0.569	1.08%								
	3	1.867	54.561	2.446	52.694	0.579	1.10%								
1° Forming	4	1.850	51.968	1.887	50.118	0.037	0.07%			64	0.08%	0.0512	1.4694	75.53	1.91%
	5	1.859	44.721	1.896	42.862	0.037	0.09%								
2° Forming	6	1.868	55.385	1.911	53.517	0.043	0.08%	2.11	37.69	35.58	0.08%	0.0288	1.4252	37.97	3.62%
	7	1.846	53.197	1.888	51.351	0.042	0.08%								
Left Bank	8	1.848	44.456	1.883	42.608	0.035	0.08%	0.89	3.94	3.05	0.09%	0.0026	1.4226	34.93	3.91%
	9	1.839	47.152	1.879	45.313	0.040	0.09%								
Right Bank	10	1.846	51.246	1.880	49.400	0.034	0.07%	0.89	7.72	6.83	0.07%	0.0047	1.4179	28.10	4.80%
	11	1.840	52.125	1.875	50.285	0.035	0.07%								
Vacuum #1	12	1.847	48.740	1.901	46.893	0.054	0.12%	6.25	15.11	8.86	0.12%	0.0105	1.4074	19.25	6.81%
	13	1.842	50.001	1.901	48.159	0.059	0.12%								
Vacuum #2	14	1.860	49.175	1.899	47.315	0.039	0.08%	5.78	9.56	3.78	0.09%	0.0033	1.4041	15.48	8.32%
	15	1.852	49.124	1.895	47.272	0.043	0.09%								
Vacuum #3	16	1.839	40.264	1.873	38.425	0.034	0.09%	5.78	8.82	3.04	0.09%	0.0026	1.4015	12.44	10.13%
	17	1.847	42.808	1.881	40.961	0.034	0.08%								
Sheet	18	1.828	95.142	10.699	93.314	8.871	9.51%	4.06	17.90	13.84	10.13%	1.4015	Losses: (included in 2° f.roll)		
	19	1.840	73.620	9.421	71.780	7.581	10.56%						0.0154	2.00	
	20	1.860	132.128	14.483	130.268	12.623	9.69%								
	21	1.829	98.620	12.231	96.791	10.402	10.75%								
								Total Collected (kg):		139		1.5053			
								Recovery:		98.6%		99.0%			

Date: June 16th, 1998 - expt.#2

Outer Wire Pressure: 80psi
Inner Wire Pressure: 30psi
Slice Opening: 4mm
Pump Speed: 1750rpm
Wire Speed: 1750rpm

Machine Profile	Drainage	Cumul. Drainage	Remain. Water	Sheet Consistenc
Headbox	0.00	0.00	139.48	1.08%
Forming Roll	101.58	101.58	37.89	3.62%
Blades	9.88	111.46	28.01	4.80%
1° Vacuum	8.86	120.32	19.15	6.81%
2° Vacuum	3.78	124.10	15.37	8.32%
3° Vacuum	3.04	127.14	12.33	10.13%

Notes: Using pulp recycled from the previous run today (slightly lower consistency and presumably depleted of fines).

Flow Analysis

Stream	Dish #	Dish Mass (g)	With Pulp (g)	With Dried Fibre (g)	Mass of Pulp (g)	Mass of Fibre (g)	Flow Consistency	Mass Balance: Bucket Mass (kg)	Mass Balance: With Stream (kg)	Mass Balance: Stream Mass (kg)	Fibre Balance: Stream Consistency	Fibre Balance: Stream Fibre (kg)	Sheet Progression: Remaining Fibre (kg)	Sheet Progression: Remaining Water (kg)	Sheet Progression: Sheet Consistency
Headbox	0	1.855	53.921	2.152	52.066	0.297	0.57%			141	0.58%	0.8123	0.8123	140.19	0.58%
	1	1.860	53.510	2.154	51.650	0.294	0.57%								
	2	1.873	60.344	2.216	58.471	0.343	0.59%								
	3	1.874	65.514	2.242	63.640	0.368	0.58%								
1° Forming	4	1.856	51.295	1.883	49.439	0.027	0.05%			70	0.06%	0.0394	0.7729	70.23	1.09%
	5	1.865	53.639	1.895	51.774	0.030	0.06%								
2° Forming	6	1.875	57.606	1.906	55.731	0.031	0.06%	2.11	38.65	36.54	0.06%	0.0205	0.6940	34.55	1.97%
	7	1.855	55.065	1.885	53.210	0.030	0.06%								
Left Bank	8	1.854	50.676	1.882	48.822	0.028	0.06%	0.89	2.20	1.31	0.05%	0.0007	0.6932	33.24	2.04%
	9	1.845	49.472	1.870	47.627	0.025	0.05%								
Right Bank	10	1.851	49.540	1.876	47.689	0.025	0.05%	0.89	6.51	5.62	0.05%	0.0031	0.6902	27.62	2.44%
	11	1.845	43.811	1.869	41.966	0.024	0.06%								
Vacuum #1	12	1.858	47.579	1.886	45.721	0.028	0.06%	6.25	19.39	13.14	0.06%	0.0080	0.6821	14.49	4.50%
	13	1.853	51.141	1.883	49.288	0.030	0.06%								
Vacuum #2	14	1.866	52.461	1.893	50.595	0.027	0.05%	5.78	12.55	6.77	0.05%	0.0036	0.6785	7.72	8.08%
	15	1.859	43.247	1.881	41.388	0.022	0.05%								
Vacuum #3	16	1.846	47.793	1.869	45.947	0.023	0.05%	5.78	7.92	2.14	0.05%	0.0010	0.6775	5.58	10.82%
	17	1.855	50.633	1.878	48.778	0.023	0.05%								
Sheet	18	1.839	63.086	8.686	61.247	6.847	11.18%	9.35	15.61	6.26	10.82%	0.6775	Losses: (included in 2° f.roll)		
	19	1.847	115.811	13.799	113.964	11.952	10.49%						0.0585	-0.84	
	20	1.872	78.266	9.915	76.394	8.043	10.53%								
	21	1.839	99.535	12.678	97.696	10.839	11.09%								
								Total Collected (kg):		142		0.7538			
								Recovery:		100.6%		92.8%			

Date: June 23, 1998

Outer Wire Pressure: 80psi
Inner Wire Pressure: 30psi
Slice Opening: 4mm
Pump Speed: 1750rpm
Wire Speed: 1750rpm

Notes Third use of pulp from June 16, 1998.

Machine Profile	Drainage	Cumul. Drainage	Remain. Water	Sheet Consistency
Headbox	0.00	0.00	140.19	0.58%
Forming Roll	105.70	105.70	34.49	1.97%
Blades	6.93	112.63	27.56	2.44%
1° Vacuum	13.14	125.77	14.42	4.50%
2° Vacuum	6.77	132.54	7.65	8.08%
3° Vacuum	2.14	134.68	5.51	10.82%

Flow Analysis

Stream	Dish #	Dish Mass (g)	With Pulp (g)	With Dried Fibre (g)	Mass of Pulp (g)	Mass of Fibre (g)	Flow Consistency	Mass Balance: Bucket Mass (kg)	Mass Balance: With Stream (kg)	Mass Balance: Stream Mass (kg)	Fibre Balance: Stream Consistency	Fibre Balance: Stream Fibre (kg)	Sheet Progression: Remaining Fibre (kg)	Sheet Progression: Remaining Water (kg)	Sheet Progression: Sheet Consistency
Headbox	0	1.868	52.398	2.141	50.530	0.273	0.54%			141	0.56%	0.7866	0.7866	140.21	0.56%
	1	1.856	63.642	2.203	61.786	0.347	0.56%								
	2	1.855	59.609	2.185	57.754	0.330	0.57%								
	3	1.856	64.730	2.207	62.874	0.351	0.56%								
1° Forming	4	1.867	49.568	1.890	47.701	0.023	0.05%			70	0.05%	0.0318	0.7548	70.25	1.06%
	5	1.866	51.145	1.887	49.279	0.021	0.04%								
2° Forming	6	1.869	48.239	1.893	46.370	0.024	0.05%	2.11	36.74	34.63	0.05%	0.0179	0.7105	32.80	2.12%
	7	1.869	52.518	1.895	50.649	0.026	0.05%								
Left Bank	8	1.871	46.120	1.892	44.249	0.021	0.05%	0.89	2.00	1.11	0.05%	0.0005	0.7099	31.69	2.19%
	9	1.856	50.625	1.881	48.769	0.025	0.05%								
Right Bank	10	1.879	45.843	1.901	43.964	0.022	0.05%	0.89	6.24	5.35	0.04%	0.0024	0.7075	26.34	2.62%
	11	1.863	53.564	1.883	51.701	0.020	0.04%								
Vacuum #1	12	1.866	59.418	1.903	57.552	0.037	0.06%	6.25	18.50	12.25	0.07%	0.0080	0.6995	14.10	4.73%
	13	1.842	50.139	1.874	48.297	0.032	0.07%								
Vacuum #2	14	1.868	46.483	1.891	44.615	0.023	0.05%	5.78	12.39	6.61	0.05%	0.0033	0.6962	7.49	8.50%
	15	1.849	50.046	1.873	48.197	0.024	0.05%								
Vacuum #3	16	1.852	48.126	1.876	46.274	0.024	0.05%	5.78	7.98	2.20	0.05%	0.0011	0.6950	5.29	11.60%
	17	1.884	53.745	1.911	51.861	0.027	0.05%								
Sheet	18	1.861	103.423	13.829	101.562	11.968	11.78%	4.06	10.05	5.99	11.60%	0.6950	Losses: (included in 2° f.roll)		
	19	1.868	69.592	9.347	67.724	7.479	11.04%						0.0265	2.83	
	20	1.856	79.211	11.007	77.355	9.151	11.83%								
	21	1.854	64.654	9.237	62.800	7.383	11.76%								
								Total Collected (kg):		138		0.7601			
								Recovery:		98.0%		96.6%			

Date: June 25, 1998

Outer Wire Pressure: 80psi
Inner Wire Pressure: 30psi
Slice Opening: 4mm
Pump Speed: 1750rpm
Wire Speed: 1750rpm

Machine Profile	Drainage	Cumul. Drainage	Remain. Water	Sheet Consistency
Headbox	0.00	0.00	140.21	0.56%
Forming Roll	107.46	107.46	32.75	2.12%
Blades	6.46	113.92	26.29	2.62%
1° Vacuum	12.25	126.17	14.04	4.73%
2° Vacuum	6.61	132.78	7.43	8.50%
3° Vacuum	2.20	134.98	5.23	11.60%

Notes: Fourth use of pulp from June 16, 1998.

Appendix C: Operator's Guidelines

This is a brief overview of what is required to safely and properly operate the laboratory scale twin-wire sheet former. Any common sense lab safety protocols, if not mentioned here, should be assumed.

Avoid wearing loose clothing that may get caught in the rolls and wires. Always wear safety boots and glasses and ear protection while running the apparatus.

When filling the headbox section, open both air purge valves; only close them when water begins to escape or the pump is started up. The pulp should be thoroughly broken up and dispersed in the reservoir WITH ONLY THE MIXERS. Never turn on the pump before the pulp has been broken down into tiny bundles. Large chunks of fibres may damage the impellers or jam the valve. Make sure the baffle bucket is in position before filling the reservoir. When ramping the pump up to full speed, proceed slowly but steadily. Sudden changes in flow rate may strain the valve and the piping.

Thoroughly wet the wires and the rolls before activating the drainage section. Also, make sure all the white water containers and the sheet container are securely in position, and that the plastic barrier is in position. Set the wires moving at the slowest speed, then set the air pressure in the pistons to the desired levels. Slowly and smoothly accelerate the wires to their operating speed. Make sure that the experiment is ready to begin, as the remaining procedures must be carried out in as short a time as possible. Quickly, set the compressed air flow rate to the blow pipe to the desired level, activate all the vacuum cleaners, and switch the headbox valve. The blow pipe and vacuum boxes will quickly remove all the lubricating water from the wires, so the goal is to get the pulp flowing into the machine to provide lubrication again as rapidly as possible.

Never leave the system unattended while it is in operation. One or more of the white water containers may need replacing mid-operation, so pay attention to their water levels. The blow pipe air flow rate may also need fine adjustment to properly place the wet sheet in the collection tank. Never allow the reservoir to empty or the pump to run dry. This would destroy the pump.

Once the desired mass of pulp has been delivered, quickly switch the valve and simultaneously begin slowing down both the pump and the wires as quickly as possible. Once both motors have reached their slowest speed, turn off all the vacuum cleaners and the blow pipe air flow. If no more experiments are to be performed, release the compressed air in the pistons (with ear and eye protection). Shut down the pump, open both purge valves, and begin draining the headbox section. Hose down the drainage section while the wires are still turning slowly, in order to remove all residual fibre. Shut down the drainage section. When the headbox section has completely drained, fill it up again with water, then open the valve and allow the water to drive out the residual pulp remaining in the headbox line. Hose down the forming roll area again, where much of this residual pulp will deposit. Allow the rest of the water to drain out. If no more experiments will be performed for a long time, remove the pipe connecting the reservoir to the inlet of the pump to allow the inside piping to air dry.

Appendix D: Project Expenses and Equipment Specifications

(All figures are reported in Canadian dollars and span the period from 1996 to 1998)

Drainage Section (total: 18 270$)

System construction, including parts and labour (by Atelier Rouleau Inc.): 16 800$

Transportation of apparatus from Atelier Rouleau to McGill (by Kings Van Lines): 750$

Construction of roll with grooves (by Atelier Rouleau Inc.): 720$

Headbox Section (total: 11 874$)

System construction, including materials and labour (by Paprican machine shops): 5000$

Peerless centrifugal pump, ANSI 8196, 1800 rpm, 2x3-6 STP: 1800$
- mechanical seal and kit: 478$
- base, safety guard and mounting: 625$

General Electric motor (extra severe duty), high efficiency, 1.15 service factor, cast iron construction, capable of 4:1 speed reduction, with a maximum of 125% of nominal speed, 3 HP, 575/3/60 volts, 1800 rpm, frame:182T (shaft 11/8"): 416$

Reliance variable speed drive, #SP500, 1SU51003, NEMA 1 enclosure, 3HP 575V, Features: start/stop-reset, program mode, forward/reverse, display of motor rpm, % load and output voltage: 1173$

Mixer impellers, model A-310: 180$

Addition of flange to pump feed pipe (by Atelier Rouleau Inc.): 865$

3-Way ball valve, 2-inch diameter, Marwin model 3L-3600, 316 stainless steel body and trim, Teflon seats, L-port, threaded ends, Cv 112, C/W double acting pneumatic actuator, Bray model 90-1180: 1240$
- Bray series 60 solenoid valve, 120 VAC, NEMA 4: 218$
- Bray series 50 limit switch, NEMA 4, (2) PSDT: 229$
- Bray series 65 positioner, 4-20 mA signal: 1450$